5-2020

Computational Study of Novel FxBN Spin Trap Analogs with Hydroxyl Radicals

Alexis Harvey

Computational Study of Novel FxBN Spin Trap Analogs with Hydroxyl Radicals

Submitted in partial fulfillment of undergraduate honors requirements

Submitted By:

Alexis K. Harvey

Honors College

University Honors Scholar

Chemistry, Honors-in-Discipline

East Tennessee State University

_____

Dr. Scott Kirkby, Research Mentor

_____

Dr. Frank Hagelberg, Second Thesis Reader

ABSTRACT

Free radicals are reactive molecules, which makes them difficult to study. Learning more about free radicals is necessary since they are implicated in many diseases and conditions such as Alzheimer's disease and ageing. Spin traps are molecules that can be used to stabilize free radicals to allow time for the free radicals to be characterized. The purpose of this research was to examine four novel spin traps that combine the properties of existing spin traps to possibly create more effective spin traps. The four novel molecules in question were designed by taking the 4-methylfuroxanyl ring from the α(Z)-(3-methylfuroxan-4-yl)-*N*-t-butylnitrone spin trap and combining it with the 5,5-dimethylpyrroline-*N*-oxide, the 5-methyl-,5-(trifluoromethyl)pyrroline-*N*-oxide, the 5-acetamide,5-methylpyrroline-*N*-oxide, and the 5-carboxamide,5-methylpyrroline-*N*-oxide spin traps. These four novel spin traps were studied using the hydroxyl radical since it is an abundant free radical in biological systems. The computational methods Hartree-Fock (HF) and Density Functional Theory (DFT) were used to calculate the optimized geometries for the reactant species and the hydroxyl radical additions at the C-site, at the O-site, and for the diadduct, which is when two free radicals add, at the HF/6-31G*, HF/cc-pVDZ, DFT/B3LYP/6-31G*, and DFT/B3LYP/cc-pVDZ levels of theory. From these calculations, the thermodynamic stability of the final product versus the initial reactants was obtained. The C-site addition was found to be more thermodynamically favorable for all the molecules than the O-site addition. The diadduct radical addition for the four molecules was the most thermodynamically favorable. The next step in the research would be to explore the methylfuroxan-4-yl ring on other molecules to continue expanding the effectiveness of spin traps, so free radicals can be better understood.

ACKNOWLEDGEMENTS

I would like to thank Dr. Scott Kirkby for introducing me to physical chemistry and for mentoring me throughout this research process. I would like to thank my second thesis reader, Dr. Frank Hagelberg. I am also grateful for the ETSU Department of Chemistry for the opportunity to do research and for my chemistry education. I would also like to acknowledge the ETSU's Honors College for funding this project through ETSU's Student-Faculty Collaborative Grant and for funding my aspirations through the University Honors Scholarship. I would like to acknowledge the Ronald E. McNair Program for funding through the Academic Year Internship and for informing me about graduate school through the Pre-Research Internship. Finally, I would like to thank my friends and my family for their unwavering support.

TABLE OF CONTENTS

LIST OF TABLES

LIST OF FIGURES

CHAPTER 1

INTRODUCTION

Free Radicals

Free radicals are molecules with at least one unpaired electron.[1] Since not all the atoms in a free radical have electrons in pairs or bonds, they are unstable. This lack of stability often makes them highly reactive.[1] Since they react so quickly, it is hard to isolate free radicals by themselves since they will react with other molecules to gain stability. Free radicals are of interest since there are many present in the body, and their high reactivity can damage biomolecules.[2] The most common ones present are reactive oxygen species (ROS).[3] Reactive oxygen species have the unpaired electron on the oxygen. Ground state molecular oxygen is a triplet, (i.e. it has two unpaired electrons in its outer shell). If the molecule is excited to a singlet state, it may become a reactive species that will then form a radical through the loss of the excited electron.[4]

The body has natural ways of dealing with free radicals, but when these natural ways become imbalanced, oxidative stress can occur. Oxidative stress occurs when there is an imbalance between the number of ROS and the available antioxidants, which neutralize ROS through oxidation-reduction reactions, or available enzymes that destroy free radicals such as super oxygen dismutase.[4,5] Some common ROS in the body include superoxide, hydroxyl, and peroxyl.[6] Superoxide is a notable ROS since it can create hydroxyl, peroxyl, and other free radicals in the body.[4,7]

Free radicals like ROS are implicated in many diseases and conditions due to their high reactivity.[2] This reactivity can be measured using half-life. Half-life is the time that it takes for half of a substance to react.[8] For example, the hydroxyl radical has an *in vivo* half-life of 10^{-9} s,

or one billionth of a second.[9] A short half-life indicates that free radicals to react close to their site of generation in the body, so they will react with biological molecules including DNA, proteins, and lipids. The reaction with DNA can cause mutagenesis, and if the mutation affects a part that codes for cell growth, it may lead to cancer.[9] A major ROS in this damage is hydroxyl.[9] ROS can also react with the side chains of amino acids in proteins. This changes the functions of proteins, which can play a part in diseases like Alzheimer's.[10] ROS have also been linked to aging since the body accumulates oxidative damage over time, and this damage could explain effects that are seen with age such as the lipid peroxidation of membranes and the decline of mitochondrial function.[11] These are some of the reasons why ROS have been implicated in many diseases and conditions.

Free Radical Reactions

Free radicals are created through both internal and external mechanisms. The external methods include cigarette smoke, ultraviolet light, and industrial chemicals.[12] The internal mechanisms include normal metabolic processes and reactions involving iron and other transition metals.[12] The reaction involving iron is known as the Fenton Reaction, and it is an important generator of hydroxyl radicals.[13,14] Another reaction involving the formation of hydroxyl radicals is the Haber-Weiss reaction, which has to use a metal catalyst like iron in biological systems for it to occur.[15,16] The focus here is on the hydroxyl radical formation since it is a strong oxidant and one of the most biologically active free radicals.[4,17]

The overall Fenton reaction is shown below in Equation 1-1. It involves the formation of a hydroxyl radical and hydroxide ion by splitting hydrogen peroxide and oxidizing iron.[18] This reaction is of biological significance since iron is present in the body, and it is a major producer

of the hydroxyl free radical.[19] Other low valent transition metals can undergo Fenton-like chemistry. Examples are vanadium and copper. [14,20,21]

$$Fe^{2+} + H_2O_2 \rightarrow Fe^{+3} + OH^{\cdot} + OH^{-} \qquad (1\text{-}1)$$

The general Haber-Weiss reaction is shown below along with the steps in Equations 1-2 to 1-4. It involves the superoxide ion reacting with hydrogen peroxide to produce singlet dioxygen, a hydroxyl radical, and a hydroxide ion.[22] In order for it to happen in biological systems, it has to be catalyzed with a metal like iron.[15] The steps of this are shown below. The second step involves the Fenton reaction, which is discussed above. The Haber-Weiss reaction is a specific example of how iron can react with not only hydrogen peroxide to produce free radicals. It can also react with the superoxide radical.[23]

$$Fe^{3+} + O_2^{\cdot -} \rightarrow Fe^{2+} + O_2 \qquad (1\text{-}2)$$

$$Fe^{2+} + H_2O_2 \rightarrow Fe^{3+} + OH\text{-} + OH\cdot \text{ (Fenton reaction)} \qquad (1\text{-}3)$$

$$\text{Net Reaction: } O\cdot_2^{-} + H_2O_2 \rightarrow O_2 + OH^{\cdot} + OH^{-} \qquad (1\text{-}4)$$

Spin Traps

Spin traps are molecules that stabilize free radicals, so they can be studied. The effects of free radicals are easy to detect, but the free radicals themselves are harder to characterize due to low concentrations and short half-lives.[24] Free radicals need to be characterized to better understand the effects that they have on the body. Electron paramagnetic resonance (EPR) spectroscopy is used in conjunction with spin trapping to study the identity and intermediacy of radicals.[25] Unlike redox reactions which eliminate free radicals, spin traps stabilize radicals as spin adducts. Due to spin traps enabling the preservation of unpaired electrons, spin adducts are still EPR active.[5] Information obtained from the spectra include hyperfine splitting constants and the g factor.[26] The g factor is similar to the chemical shift in nuclear magnetic resonance (NMR)

spectroscopy since it is dependent on the chemical environment, which means the shift of the g factor will reveal information about the chemical environment of the unpaired electrons.[26] The hyperfine splitting constants also reveal information about the chemical environment since the splitting occurs due to interactions between the unpaired electron spin and the nuclear spin.[26,27] Both the g factor and the hyperfine splitting constants are dependent on each specific radical, and it is how the free radicals can be characterized. Spin trapping can also be paired with immunoassays to characterize free radicals.[28,29] This method is fairly new, and it is being explored more since biochemists, who are the most interested in biological systems with free radical damage, are more familiar with immunoassays than EPR spectroscopy.

Effective spin traps need to possess several characteristics like stability, water solubility, lipophilicity, low cytotoxicity, resistance to bioreduction, and possession of a unique EPR spectrum for each different spin adduct.[30] Water solubility ensures the usage of spin traps in biological systems since they are aqueous in nature. Cytotoxicity must also be considered for biological systems, so the cells will not die. Lipophilicity is important if the spin traps need to cross the lipid membrane of cells. The spin adducts that form need to be thermodynamically stable. If the spin adducts decay too quickly due to having short half-lives from being unstable, they will not be able to be detected. This concept ties into the idea of resisting bioreduction since the spin adducts need to be stable in their radical form, so their unpaired spin will be detectable. They also need a unique EPR spectrum, so the radicals can be characterized. The spin trap and radical reactions should also be kinetically favorable to ensure that a lower concentration of the spin trap will be needed, which would prevent possible cytotoxicity from large doses.[31]

Free radicals are captured by spin traps using radical addition reactions instead of radical coupling or bimolecular homolytic substitution reactions. A radical addition reaction is a

requirement for a viable spin trap since the free radical should be captured and not destroyed. Radical coupling would destroy the free radical since it involves two radicals coming together to form a closed shell species, which is one that does not have an unpaired electron.[1] Biomolecular homolytic substitution involves the radical abstracting a hydrogen from a molecule and leaving the molecule that the hydrogen was abstracted from as the radical.[1] This reaction would destroy the radical of interest while creating a new radical. On the other hand, a radical addition reaction involves an electron-poor free radical adding to an electron rich double or triple bond. This addition causes a bond to form between the free radical being added, and an atom in the molecule being added to.[1] This reaction is the one that is needed since the free radical of interest is still in its original form, and the product that is created is EPR active due to the unpaired electron. These facts allow the original free radical to be identified and characterized.[26]

Current spin trap classes include nitrones and nitrosos.[32] Two common nitroso spin traps are 2-methyl-2-nitrosopropane (MNP) and 3,5-dibromo-4-nitrosobenzenesulfonic acid (DBNBS).[33] Two common nitrone spin traps are α-phenyl *N*-t-butyl nitrone (PBN) and 5,5-dimethylpyrroline *N*-oxide (DMPO).[33] These four spin traps are shown below.

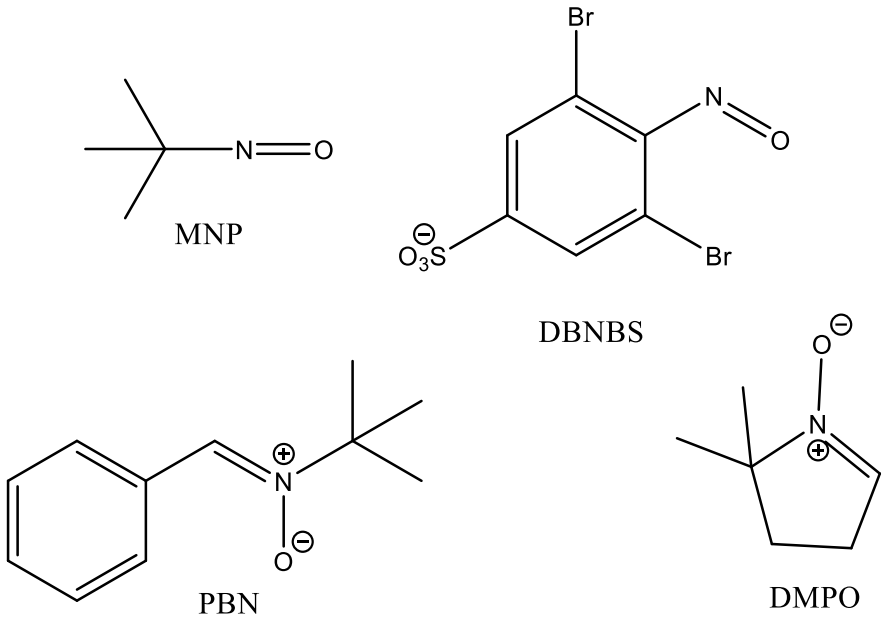

Figure 1.1. Structures of the two most common nitroso spin traps: 2-methyl-2-nitrosopropane (MNP) and 3,5-dibromo-4-nitrosobenzenesulfonic acid (DBNBS), and the two most common nitrone spin traps: α-phenyl *N*-t-butyl nitrone (PBN) and 5,5-dimethylpyrroline *N*-oxide (DMPO).

Nitroso spin traps are more toxic and more unstable than nitrones, which makes nitrones the more widely used class of spin traps.[33,34] Consequently, research on nitrosos has been limited even though they produce sharper EPR spectrums than nitrones since the free radical binds to the nitrogen and the unpaired electron goes to the adjacent oxygen, and it causes the EPR features to be distinct.[33,35] Nitrones produce worse EPR spectra than nitrosos since their spin adducts can be reduced to their hydroxylamine derivatives, which is shown in Figure 1-2. These derivatives are EPR inactive since they no longer contain an unpaired electron.[36] Hydroxylamine derivatives can also be oxidized to produce a false positive result. This is rare under mild, biological conditions, but the possibility does exist.[37,38]

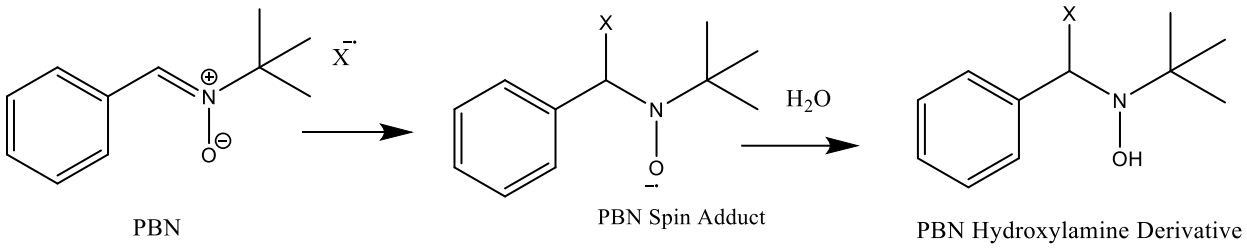

Figure 1.2. The reduction of α-phenyl *N*-t-butyl nitrone (PBN) to its hydroxylamine derivative. The first step results in the formation of the PBN spin adduct with a generic free radical. The second, is the reduction of the free radical on the oxygen to a hydroxy group.

Nitrones also produce less clear EPR spectra than nitrosos since the addition of the free radical to the C-site, or at the carbon attached to the N-C double bond, is distant from the unpaired electron on the oxygen. This causes the hyperfine splitting to be less clear.[39] Despite these drawbacks, nitrones are still the most commonly used class since they are more stable and less toxic than nitrosos.[33,34]

Nitrone spin traps react to form nitroxide spin adducts. Radical addition to the nitrone is favored at the carbon, or C-site (see Figure 1.3). The oxygen, or O-site, is favored for a second addition, leading to the formation of a diadduct, which is two free radical additions.[40] In a viable spin trap, the radical must add to the spin trap instead of taking, or abstracting, a hydrogen. Nitrones work well since the addition of the free radical is favored over the abstraction of a hydrogen unlike other functional groups, which include imines and aldehydes.[41] The order of radical reactivity with nitrones from least to most favorable is nitroxide, superoxide, peroxide, methyl, and hydroxide.[42] Hydroxide, the most favorable free radical, is the radical of interest for this study since as mentioned previously it is one of the more prevalent free radical species.

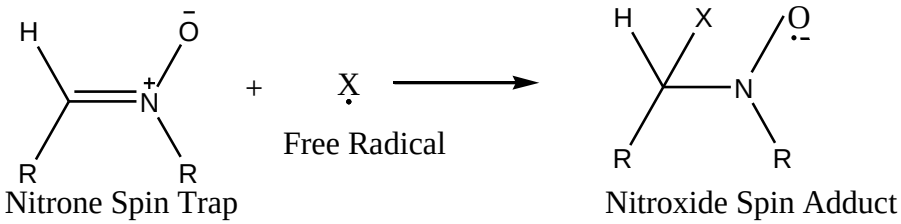

Figure 1.3. The general reaction is of a nitrone and a free radical adding at the carbon, C-site, to form the nitroxide spin adduct is shown in the above reaction.

DMPO

5,5-dimethylpyrroline-*N*-oxide (DMPO) is the cyclic, ring-based, prototype for nitrones. It has been a mainstay due to its clear EPR spectrum.[6] Another important characteristic of DMPO is that it can react with oxygen centered and carbon centered free radicals.[43] Selectivity of the radical addition matters when determining what specific radicals need to be trapped. One limitation for DMPO is that the adducts are not stable, so their half-lives are short. For example, the half-life of the DMPO superoxide adduct is one minute, so the intensity of the signal is too low for the actual amount of superoxide in the system.[44] Another limitation for DMPO is that its superoxide adduct decomposes into the hydroxide adduct.[45] This means that the amount of superoxide cannot be accurately measured since the superoxide adduct will form the hydroxide adduct.

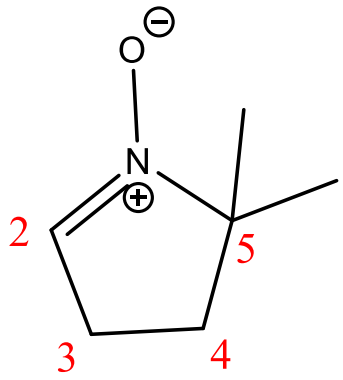

Figure 1.4. The above structure is for 5,5-dimethylpyrroline-*N*-oxide (DMPO), the prototype cyclic nitrone spin trap. The carbons are labeled by how they will be referenced throughout the discussion.

DMPO has both positive and negative attributes as a spin trap as discussed previously. To negate the negatives, substituted analogs have been explored. Substituted DMPO molecules are promising since they were shown to have a two-fold increase in the rate of reaction meaning that they are more sensitive to free radicals precent.[31] In the substituents being explored, it is important to note that bulky substituents do not prevent reduction to the hydroxylamine product from happening, especially not without sacrificing spin trap capabilities.[46] Reduction is important to consider since it can make the spin trap EPR inactive. On the other hand, electron withdrawing groups were found to positively affect the reactivity of the spin trap. Charges and intramolecular hydrogen-bonding also positively affect the spin adduct stability.[31] Reactivity is important in increasing the sensitivity of the spin trap, and stability is important in obtaining EPR readings.

Several studies have been done on DMPO substituted derivatives and electron withdrawing groups that affects the reactivity. Villamena *et al.* found that an amide group at the C-5 position, which is labeled on the DMPO molecule above, increases the positive charge of the

nitronyl carbon, and therefore gives it an enhanced reactivity towards superoxide radical when compared to the original DMPO parent molecule. Increasing the positive charge of the nitronyl carbon can be done using other electron withdrawing groups. Consequently, Villamena *et al.* found that 5-carboxamide,5-methylpyrroline-*N*-oxide (AMPO), 7-oxa-1-azaspiro[4.4]non-1-en-6-one 1-oxide (CPCOMPO), 5-methyl-,5-(trifluoromethyl)pyrroline-*N*-oxide (TFMPO), 5-acetamide,5-methylpyrroline-*N*-oxide (MAMPO), and 5-acetamide,5-acetyloxypyrroline-*N*-oxide (EMAPO) increase the efficiency of superoxide trapping.[47] These molecules all contain electron withdrawing groups. Additionally, Han *et al.* found that the beta-cyclic nitrone 5-*N*-β-cyclodextrin-carboxamide-5-methyl-1-pyrroline *N*-oxide (Beta-CDMPO), which has an amide linker group, also shows a higher rate of superoxide trapping and stability when compared to DMPO, 5-(ethoxycarbonyl),5-methyl-1-pyrroline-*N*-oxide (EMPO), and 5-(diethoxyphosphoryl),5-methyl-1-pyrroline-*N*-oxide (DEPMPO). It was concluded that the amide linker group led to these characteristics.[48] A limitation of the amide group is the hydrophilicity. Spin traps need to exhibit amphiphilicity to be the most effective in biological systems.[49] Further developments of spin traps need to account for this consideration.

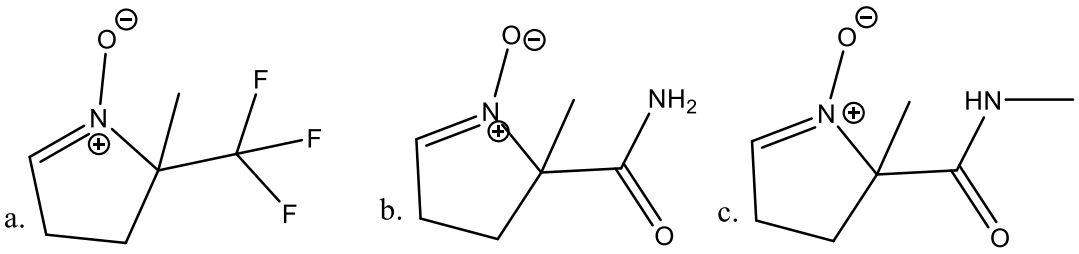

Figure 1.5. The structures for three substituted DMPO analogs: a. 5-methyl-,5-(trifluoromethyl)pyrroline-*N*-oxide (TFMPO), b. 5-carboxamide,5-methylpyrroline-*N*-oxide (AMAPO), and c. 5-acetamide,5-methylpyrroline-*N*-oxide (MAMPO).

Several studies have also been done on DMPO substituted derivatives looking at the effects of charge and intramolecular H bonding on spin adduct stability.[50] The more negative the nitrogen and the more positive the carbon, the stronger the carbon-nitrogen bond which leads to more stable spin adducts. C-2 substituents do not influence the stability due to charge as much as substituents that affect the charge density on the C-5 and the nitrogen.[50] Villamena *et al.* found that the more positive the charge density on the nitronyl C, the more stable the spin adduct. Sulfonated nitrones have the highest positive charge density, but sulfonyl groups react with hydroxyl radicals to form carbon centered radicals.[50] This means that other groups that lead to higher positive charge density need to be explored. For example, fluoride substituents lead to more stable spin adducts due to the inductive effects making the C more positive.[51] In a separate study, Villamena *et al.* explored the addition of the peroxyl radical. The *N*-monoalkylamide nitrones MAMPO and EMAPO are not thermodynamically favored for peroxyl radical addition, but EMPO and TFMPO are thermodynamically favored for peroxyl radical addition. There is no generally accepted explanation since there was no correlation between the electronegativity of the atoms and the favor to radical addition. There is evidence that strong H-bonding increases the stability of the spin adduct, which can ease the addition of the peroxyl radical.[50,52]

PBN

The linear prototype for nitrone spin traps is α-phenyl *N*-t-butyl nitrone (PBN), and it has not been studied as much as DMPO since it does not give as clear hyperfine splitting constants for the EPR spectra.[32] PBN does form a stable spin adduct, so even though its EPR spectra are not as clear there is still value in it being explored further.[1] Other characteristics in PBN's favor are that it is stable under UV irradiation, and it is selective towards carbon centered spin adducts.[43]

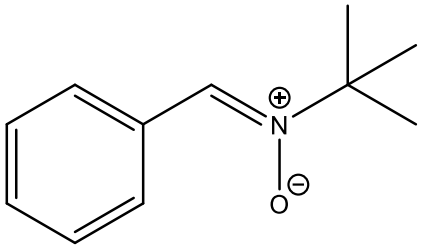

Figure 1.6. The structure of α-phenyl *N*-t-butyl nitrone (PBN); the prototype linear nitrone spin trap.

Several studies exploring PBN analogs have been conducted. Rosselin *et al.* studied the polar effects of para-substituents on PBN and its electrochemical properties. It was concluded that electron withdrawing groups increase the ease of oxidation, which is correlated with increased antioxidant abilities.[53] In another study, Rosselin *et al.* found that hydroxyl groups increase water solubility with up to two groups on the tert-butyl group of PBN. Having more than two substituents on PBN tert-butyl group decreases the reactivity. Ester compounds show higher rates of lipophilicity, but they are the least water soluble. Overall, the amide linker group was found to be the most viable for use in biological systems.[54] Conversely, para-substituting PBN's benzyl ring with carboxylic acid increases spin trapping whereas the amide group decreases spin trapping.[55]

Cyclic derivatives of PBN function as more efficient spin traps and antioxidants than the parent PBN.[56] One studied by Porcal *et al.* synthesized thiadiazolyl and furoxanyl ring analogs of PBN to test for their spin trapping abilities. They were found to be effective at radical scavenging and non-toxic.[57] Seven of these were chosen to be further studied including α(Z)-(3-methylfuroxan-4-yl)-*N*-t-butylnitrone (FxBN). FxBN is a PBN analog substituted with a 4-furoxanyl ring.

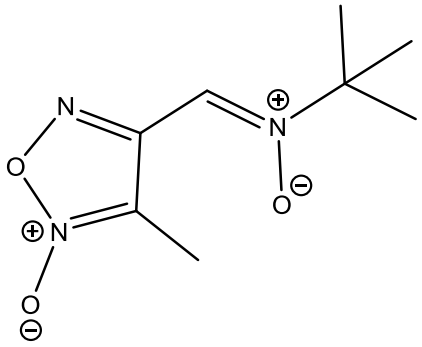

Figure 1.7. The structure of α(Z)-(3-methylfuroxan-4-yl)-N-t-butylnitrone (FxBN).

Overall, FxBN was found to be more effective than PBN and DMPO in its spin trapping abilities. Important data to support this conclusion is the comparison of half-lives. The FxBN-hydroxide radical spin adduct had twice the half-life of the DMPO-hydroxide adduct and two hundred times the half-life of PBN-hydroxide adduct in a biological environment.[58] The half-life for FxBN superoxide radical is thirty times the value for the DMPO superoxide radical.[58]

PBN and its derivatives have been explored for medicinal uses. Since it is both hydrophilic and lipophilic, it can cross the blood brain barrier.[59] PBN increases cognitive performance and the lifespan in aging rats due to its antioxidant abilities.[60] Trapping of a radical is not as efficient as redox reactions when preventing lipid peroxidation signifying that PBN does not therapeutically act as a spin trap.[56] This is beneficial since high doses of PBN are required to therapeutically act as a spin trap.[61] The analog 4-[[(1,1-dimethylethyl)oxidoimino]methyl]-1,3-benzenedisulfonic acid (NXY-059) was the medicinal version of PBN brought through clinical trials.[62] NXY-059's main action was not radical trapping but inhibiting the pathway for nitric oxide production.[63] In clinical trials in humans, it was not proven to significantly improve outcomes in stroke patients.[32] Other possible nitrones should be explored for both their spin trapping and antioxidant properties.

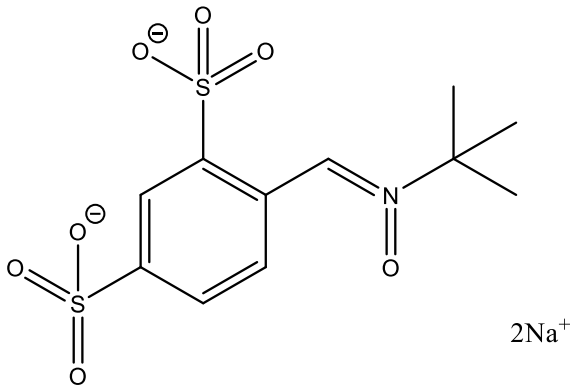

Figure 1.8. The structure of (NXY-059), the α-phenyl *N*-t-butyl nitrone (PBN) analog brought through medicinal clinical trials.

CHAPTER 2

QUANTUM MECHANICS

Basics of Quantum Mechanics

In the late 19th century, classical mechanics was used to describe the macroscopic world, but there were problems that it could not solve that arose from the microscopic world. Two of these issues were black body radiation and the photoelectric effect.[64] Classical mechanics predicted that a black body, an object that absorbs all light incident on it, should emit light, known as black body radiation, with infinite intensity at higher frequencies. Since this phenomenon could not occur, it was known as the ultraviolet catastrophe. Planck explained black body radiation by discovering that energy is in emitted in discrete or quantized packets that can be described using a constant. This constant would come to be known as Planck's constant (h).[65] The specific levels of energy is where quantum mechanics derives its name from since "quanta" means packet.[64] The formula derived from this idea is below where E represents energy, h is Planck's constant, and ν is the frequency of the light represented as a wave.[66]

$$E = h\nu \qquad (2\text{-}1)$$

Albert Einstein was the first to describe the photoelectric effect, and it further proved Planck's findings since the Plank constant could be used to describe it, too.[67] The photoelectric effect is observed when a certain frequency of light hits a metal, and electrons are ejected. Classical mechanics predicted that it would be the number of photons that hit a piece of metal, or intensity of light, that would affect the amount of the electrons that were emitted. In actuality, it is the frequency, or the energy, of the photons that affects the electrons that are initially ejected. This specific frequency is determined by the minimum energy needed to extract electrons from a metal, which is known as the work function of the metal. Once the certain energy of light is achieved, the electrons are emitted based on the intensity of light.[64] The equation that describes this relationship is below. Where KE is kinetic energy, h is Planck's constant, ν is the frequency, and $\phi = h\nu_0$, where ϕ is the work function and ν_o the minimum frequency that induces the photoelectric effect .[64]

$$KE = h\upsilon - \phi \qquad (2\text{-}2)$$

Bohr created a model of the atom that included quantized variables. He concluded that electrons must occupy specific energy levels around the nucleus. If this was not the case, the negative electrons would spiral into the positive nucleus, and therefore, atoms would not be able to exist.[67] His model is accurate in describing the fact that electrons are quantized, but it is inaccurate in operating with well-defined electron trajectories. In fact, the locations of electrons must be described in terms of the probability density. The probability density measures the probability of an electron occupying a specific position in space.[60] The probability comes from the wave function, and the probability density is described using quantized electron orbitals.[68]

The Heisenberg Uncertainty Principle states that the universe is probabilistic not deterministic since there is uncertainty in the simultaneous measurement of certain properties of

particles. One form of the Heisenberg Uncertainty Principle can be stated formally in Equation 2-3. This equation means that the more that is known about the momentum the less that will be known about the particle's position.[64] This is not due to poor measuring capabilities. Instead, it is due to the inherent uncertainty introduced by the act of measuring.

$$\Delta x \Delta p_x \geq \frac{\hbar}{2} \qquad (2\text{-}3)$$

Besides the quantized energy levels, another important concept in quantum mechanics is that matter can act as both a particle and a wave. Wave-particle duality was discovered in experiments involving the photoelectric effect and particle interference.[67] The phenomenon is demonstrated very clearly by the double slit experiment. This experiment involved particles going through a slit, and then going through a double slit. The particles created a diffraction pattern, which occurs when waves undergo destructive and constructive interference. De Broglie interpreted related observations by introducing the relationship $\lambda = \frac{h}{p,}$, assigning a wave length λ to a particle with momentum p.[64] This duality matters when trying to understand electrons since due to their microscopic size the wave part is large enough to be detectable, so it will influence their properties.

Schrödinger Wave Equation

A fundamental postulate of quantum mechanics is the Schrödinger Wave Equation. The Schrödinger Wave Equation is derived from the classical one-dimensional wave equation using de Broglie's idea of waves and the fact that the energy of a particle consists of both potential and kinetic energy.[66] There are two versions of the Schrödinger Wave Equation—the time-dependent and the time-independent. Both can be used for chemical purposes with the focus here being on the time-independent wave equation since no calculations requiring time like molecular dynamics were calculated. The wave functions that are obtained from the time-independent wave

function are known as stationary-state wave functions since they are independent of time. The time-independent Schrödinger Wave equation is:[64]

$$-\frac{\hbar^2}{2m}\frac{d^2\psi}{dx^2} + V(x)\psi(x) = E\psi(x) \qquad (2\text{-}4)$$

The symbol $\hbar$, which is known as h bar, is the reduced Planck's constant and is equal to $\frac{h}{2\pi}$. $\psi(x)$ is the wave function of a particle, and it describes the movement of a particle in a potential energy field, V(x), and the kinetic energy is represented with $\frac{-\hbar^2}{2m}\frac{d^2}{dx^2}$. The combined potential and kinetic energy can be represented using a quantum mechanical operator known as the Hamiltonian ($\widehat{H}$). An operator describes a mathematical function that should be performed on the variables following it. The Hamiltonian operator can be defined as $\widehat{H} = \frac{-\hbar^2}{2m}\frac{d^2}{dx^2} + V(x)$, which includes both the kinetic and the potential energy terms respectively.[64]

Since the energy can be described using the Hamiltonian operator, the Schrödinger equation can be rewritten as an eigenvalue problem. This means that there is an eigenfunction and an eigenvalue.[64] The eigenfunction when acted on by an operator will give the eigenvalue. In other words, applying the operator on the eigenfunction will always give a constant, or eigenvalue, times the original function. For the Schrödinger equation, the eigenvalue formulation is below with $\psi(x)$, the wavefunction, being the eigenfunction and E, the total energy, being the eigenvalue.[64]

$$\widehat{H}\,\psi(x) = E\,\psi(x) \qquad (2\text{-}5)$$

The wave function has a probabilistic interpretation. This means that the wave function can tell the probability of where an electron is located. To determine the probability, the following interpretation of the wave function can be used: $\psi^*(x)\,\psi(x)dx$.[69] $\psi^*(x)$ is the

complex conjugate of the wave function $\psi(x)$. The physical interpretation is that the absolute square of the wave function, $\psi^*(x)\,\psi(x)$, is a probability distribution function.[64]

Since wave functions describe the probability of an electron's location, they must be normalized. To be normalized means to be set equal to one. The value is one since the particle has to exist, so the probability the particle is somewhere is one. This can be expressed in the equation below where A is the normalization constant.[64] The normalization constant is used to normalize the wave function times its complex conjugate to achieve a value of one. Often the wave function is real-valued and therefore identical with its complex conjugate. The square of this wave function will give the electron density as described earlier.[67]

$$1 = |A|^2 \int_0^a \psi^*(x)\,\psi(x)dx \qquad (2\text{-}6)$$

Another concept unique to quantum mechanics is the concept of spin. Electrons occupy specific energy levels in orbitals. These orbitals can be described using quantum numbers that include the angular momentum quantum number (l) and the magnetic quantum number (m_l). These numbers determine the shape and orientation of the orbital.[64,68] Only two electrons can occupy an orbital, and the quantum number that distinguishes these two electrons is the spin quantum number, which is 1/2. The z-component of the spin is represented as either +1/2 or -1/2.

The Pauli Exclusion Principle states that only two electrons can occupy a spatial orbital, and the two electrons must have different a different z-component of spin.[71] In other words, two electrons must differ from each other with respect to at least one quantum number. The equation that truly represents all three properties is shown below.[64] The α and β are the spin functions and represent the concept of +1/2 and -1/2 for the spin. The x, y, and z coordinates describe the position of the orbital in space.

$$\Psi(x,y,z,\sigma) = \psi(x,y,z)\alpha(\sigma)\ or\ \psi(x,y,z)\beta(\sigma) \qquad (2\text{-}7)$$

Approximation Methods

Among many others, there are four commonly used models in quantum mechanics that describe various motions. These four models are particle in a box, the harmonic oscillator, the rigid rotor, and the hydrogen-like atom. The particle in a box model describes spatially confined systems. The harmonic oscillator describes vibration. The rigid rotor describes rotation. The hydrogen-like atom describes the behavior of an electron in a bound two-body system.[64] These models are useful for understanding concepts in quantum mechanics by creating ideal situations to illustrate them. For example, the particle in box illustrates how energy levels must be quantized since the box boundary conditions impose standing-wave behavior on the wave function of the particle.[72]

The hydrogen atom is a system that can be solved exactly using the Schrödinger Equation. The hydrogen atom system is a two-body problem since it consists of a nucleus and an electron. Since there is no interelectronic repulsion term in the Hamiltonian, the wave equation can be solved exactly.[64] This system can be used to describe simple orbitals, which becomes important for understanding more complex systems that have more complex orbitals.[73] After the hydrogen atom or any other two-body problems like the helium cation, the problem becomes a three-body or greater problem. Approximation methods have to be used to calculate an approximate solution since the exact solutions of the Schrödinger equation cannot be determined due to the electron-electron repulsion term.[66] The electron-electron repulsion energy relies on knowing the location of an electron in respect to the other electrons in the system. Since only electron density can be known, it is impossible to calculate the exact value.

The helium atom is a simple example of a multi-electron system. Its Hamiltonian under the infinitely heavy nucleus approximation is below

$$\hat{H} = -\frac{\hbar^2}{2m_e}\nabla_1^2 - \frac{\hbar^2}{2m_e}\nabla_2^2 - \frac{2e^2}{4\pi\varepsilon_0 r_1} - \frac{2e^2}{4\pi\varepsilon_0 r_2} + \frac{e^2}{4\pi\varepsilon_0 r_{12}} \qquad (2\text{-}8)$$

The first two terms, $\frac{\hbar^2}{2m_e}\nabla_1^2$ and $\frac{\hbar^2}{2m_e}\nabla_2^2$, are the kinetic energy terms for the two electrons, the next two terms, $\frac{2e^2}{4\pi\varepsilon_0 r_1}$ and $\frac{2e^2}{4\pi\varepsilon_0 r_2}$, are from the potential energy of the position of each electron, and the final term, $\frac{e^2}{4\pi\varepsilon_0 r_{12}}$, is due to the electron-electron repulsion energy. This is the term described above that has to be solved using approximation methods.

Atomic units are used to simplify multi-electron equations. The atomic unit of energy is the hartree (E_h), and its value is 2625.500 kJ/mol.[64] Using atomic units, the Hamiltonian operator for a helium atom goes from the Hamiltonian shown in Equation 2-9 to the Hamiltonian shown in Equation 2-10. This example shows how atomic units can help represent equations more simply.

$$\hat{H} = -\frac{\hbar^2}{2m_e}\nabla_1^2 - \frac{\hbar^2}{2m_e}\nabla_2^2 - \frac{2e^2}{4\pi\varepsilon_0 r_1} - \frac{2e^2}{4\pi\varepsilon_0 r_2} + \frac{e^2}{4\pi\varepsilon_0 r_{12}} \qquad (2\text{-}9)$$

$$\hat{H} = -\frac{1}{2}\nabla_1^2 - \frac{1}{2}\nabla_2^2 - \frac{2}{r_1} - \frac{2}{r_2} + \frac{1}{r_{12}} \qquad (2\text{-}10)$$

Two fundamental approximation methods include the variational method and perturbation theory. The variational method takes the Schrödinger equation, $\hat{H}\,\psi(x) = E\,\psi(x)$, multiplies it by the complex conjugate of the wave function, and integrates it over all space to obtain the following equation for the ground state energy.[64]

$$E_0 = \frac{\int \psi^*_0 \hat{H}\ \psi_0 d\tau}{\int \psi^*_0\, \psi_0 d\tau} \qquad (2\text{-}11)$$

This value will be minimized within a set of parameters to obtain a value for the energy. The equation has a similar form to the expression of the expectation value since the expectation

value involves finding an average, and the goal of this is to find the average energy over the space of interest.[67]

If the wavefunction is replaced with a trial function, the following equation is obtained.[64]

$$E_{\phi} = \frac{\int \phi^* \hat{H}\, \phi d\tau}{\int \phi^* \phi d\tau} \qquad (2\text{-}12)$$

A trial function is necessary since the exact Schrödinger wave function is only known for two-body systems. This trial function is a guess of what the true wave function is.

The variational principle states that $E_{\phi} \geq E_0$. The energy for the trial function will always be greater or equal to the energy of the actual wavefunction.[64] The closer the trial function is to the wavefunction the lower the energy.[67] To find this out, parameters are set for the variational principle. These parameters can be used to minimize the trial function energy to obtain a value as close as possible to the ground state energy.[64]

Perturbation theory involves partitioning the Hamiltonian into the part that can be solved exactly and a perturbation term that cannot be solved exactly. For example, the electron repulsion term can be added as a perturbation. The perturbation should only have a small effect on the unperturbed wavefunction.[65] Due to this, the actual wavefunction can be described based off of the small changes caused by the perturbation. The following represents the unperturbed Schrödinger equation: $\hat{H}^{(0)}\psi(x)^{(0)} = E^{(0)}\,\psi(x)^{(0)}$.[64] The perturbation that will be added to the Hamiltonian will look like the following: $\hat{H} = \hat{H}^{(0)} + \hat{H}^{(1)}$, where $\hat{H}^{(0)}$ is the unperturbed Hamiltonian and $\hat{H}^{(1)}$ is the perturbation. The expressed wavefunction will then be a combination of the Hamiltonian from the unperturbed and perturbed, which can be expressed as $\psi = \psi^{(0)} + \psi^{(1)}$. There can be several perturbations added, but each addition will become less significant, so they are not exactly necessary to do.[64]

Computational Chemistry

The approximation methods described above are the basis of computational chemistry. Computational chemistry consists of four main methods.[66] These methods are molecular mechanics, *ab initio* calculations, semiempirical calculations, and molecular dynamics calculations. Molecular mechanics calculations are fast since it considers molecules as atoms attached together with springs. *Ab initio* calculations try to solve the Schrödinger equation directly, which is where the name *ab initio* comes from since it means first principles. Semiempirical calculations also try to solve the Schrödinger equation, but they are guided by experimental data. Molecular dynamics calculations involve using the laws of motion to calculate the energy for molecules.[66] For the purposes of this research, the Hartree-Fock Self Consistent Field method, which is an *ab initio* method, and Density Functional Theory will be discussed.

Hartree-Fock Self-Consistent Field Method

The Hartree-Fock Self Consistent Field (HF-SCF) method can be used to determine the wave function for a multielectron system. It involves writing the trial function in terms of orbitals. This is shown in the following relationship for the helium atom in Equation 2-13.

$$\psi(r_1, r_2) = \phi(r_1)\phi(r_2) \qquad (2\text{-}13)$$

The functions on the right side of Equation 2-14 will be the same if the electrons are in the same orbital. The potential energy for this equation can be thought of as an average potential or effective potential. This will produce an effective Hamiltonian represented as $\widehat{H}^{eff}$. [64] Equation 2-11 shows the value of the effective Hamiltonian including the effective potential energy term, V^{eff}.

$$\widehat{H}_1^{eff}(r_1) = -\frac{1}{2}\nabla_1^2 - \frac{2}{r_1} + V_1^{eff}(r_1) \qquad (2\text{-}14)$$

In the Hartree-Fock model, this depends on the wavefunction,. Problems like this are solved using a self-consistent field method. This method involves guessing a trial function to determine the effective Hamiltonian, and then, solving for the wave function. This process is continued until the output and the input are self-consistent.[64] This means that the output and the input should converge to a single value after the iterations.

The Hartree-Fock energy will not be correct since it does not account for the correlation energy. The correlation energy is the energy of interaction between the electrons because their motion is not independent. For the Hartree-Fock method, the electrons are assumed to behave independently of one another. The relationship between the correlation energy, the actual energy, and Hartree-Fock energy can be expressed through the relationship in Equation 2-15.[64]

$$CE = E_{exact} - E_{HF} \qquad (2\text{-}15)$$

To improve upon the correlation energy issue, some methods, for example the Møller-Plessett method, use perturbation theory to solve for it.[74]

The wave function for a molecule describes the position of all the electrons in the molecule, and it can be thought of as a product of the individual wave function of electrons. This is known as the Hartree product.[75] The Hartree product is derived from the idea that the energies of all of the electrons' Hamiltonians can be added together to find the total energy. Since the energies are added together, the eigenfunctions of the energies can be represented as products of the one-electron spin orbitals.[75]

Unfortunately, the Hartree product does not work since the sign does not change when electrons are switched as required by wave function antisymmetry which is based on the exclusion principle, .[64] This is important since any multielectron problem must account for this principle. The antisymmetry principle states that all electronic wave functions must change signs,

or be antisymmetric, when any two electrons switch coordinates .[64] Instead of the Hartree product, Slater determinants are used to represent the electron wave functions since they follow the antisymmetric principle.[75] The Slater determinants can be represented as $\hat{F}_i\phi_i = \epsilon_i\phi_i$. The effective Hamiltonian is called the Fock operator ($\hat{F}_i$), and the eigenvalues of ϵ_i are the orbital energies. [64]

To go from atoms to molecules, another approximation has to be used called the Born-Oppenheimer approximation. This approximation works by ignoring nuclear motion, which simplifies the Hamiltonian for a molecule. Nuclear motion can be ignored since the nucleus is so much larger than an electron it moves so much slower that it can be thought of as remaining still. Since the nuclei have "fixed," parameterized, positions, the potential energy of the electrons can be calculated in terms of the nuclei's fixed position.[66] Being able to calculate this potential energy surface is important in determining the properties of a molecule.

Molecular orbital theory is used to describe bonds for molecules. Molecular orbitals are designed in much the same way as atomic orbitals, so the quantum mechanical principles discussed earlier still apply to them. A linear combination of atomic orbitals is used to determine the molecular orbital, and then the coefficients are determined using a self-consistent field calculation.[64] The atomic functions used to construct the linear combination of atomic orbitals to make the molecular orbital is called a basis set.[64] In other words, the basis set represents the functions that will be calculated for an orbital. The larger the basis set, the more accurate the calculations are, but also the more time consuming.[75] Atomic orbitals are no longer directly represented by Slater orbitals. Instead, they are represented using Gaussian functions that describe the Slater orbitals. The atomic orbitals in a basis set are the sum of the Gaussian functions. This is represented by:[64]

$$\psi_i = \sum_{k=1}^{M} c_{ki}\phi_k \qquad (2\text{-}16)$$

The coefficient c_{ki} can be determined using a set of algebraic equations known as the Roothaan equations. The F_{ij} is the ijth matrix element of the Fock operator and S_{ij} is the overlap integral between the basis functions φ_i and φ_j:

$$\sum_{j=1}^{M}(F_{ij} - E_i S_{ij})c_{ij} = 0 \qquad (2\text{-}17)$$

Density Functional Theory

Another computational method that has been developed outside of the Hartree-Fock method is the Density Functional Theory (DFT). It is based on two mathematical theorems proved by Kohn and Hohenberg.[76] The first theorem is that "the ground state energy from the Schrödinger equation is a unique functional of the electron density."[75] A functional is a function of a function. This means another way of thinking about the first theorem is that the ground state energy can be expressed as E[n(r)] where n(r) is the electron density. Thinking of electrons in terms of density works since the exact locations of the electrons are impossible to find, but the probability of the electrons' locations, and therefore, their density is practical to find.[75] The second theorem states that "the electron density that minimizes the energy of the overall functional is the true electron density corresponding to the full solution of the Schrödinger equation."[75] A variational principle approach can be used to find the correct functional.

The functional can be written as:

$$E[(\psi_i)] = E_{known}[(\psi_i)] + E_{XC}[(\psi_i)] \qquad (2\text{-}18)$$

The known terms include electron kinetic energies and the Coulomb interactions between electrons and nuclei, between pairs of nuclei, and between the electrons. The E_{xc} part stands for the exchange-correlation energy. The issue involved in solving this is again the many-body

problem issue. Kohn and Sham solved this issue with the Kohn-Sham equations, which have the form:

$$\left[-\frac{\hbar^2}{2m}\nabla^2 + V(r) + V_H(r) + V_{XC}(r)\right]\psi_i(r) = \mathcal{E}_i\psi_i(r) \qquad (2\text{-}19)$$

The solution of the Kohn-Sham equations are single-electron wave functions that depend on only three spatial variables, $\psi_i(r)$. V(r) describes the interactions between an electron and the nuclei present in the molecule. $V_H(r)$ describes the Coulombic repulsion between an electron and the total electron density. $V_{xc}(r)$ describes the exchange and correlation contributions to the single-electron equation. This part of the equation corrects for the issue in describing V_H since the electron is also repelling itself in the current description. Since the Kohn-Sham equations depend on the solutions of these equation, a similar iterative approach is used to solve the equations like the one used in the HF-SCF.[75]

The exchange-correlation functional cannot be known, but it can be approximated. The simplest approximation used is the local density approximation (LDA). This approximation is derived from the fact that the electron density is constant in a uniform electron gas model. At each point in the uniform electron gas model, the exchange-correlation potential is set as a known potential. This method uses only the local density to approximate the exchange-correlation functional. Hence, the name of it is the local density approximation.[75] Using this approximation allows DFT to account for the electron correlation energy unlike the HF-SCF.

For this project, HF and DFT will be used to calculate the optimized geometries of the four novel spin traps. The four novel spin traps were derived from taking the 4-methylfuroxynl ring from FxBN and combining it with DMPO, TFMPO, AMPO, and MAMPO to possibly create more effective spin traps.

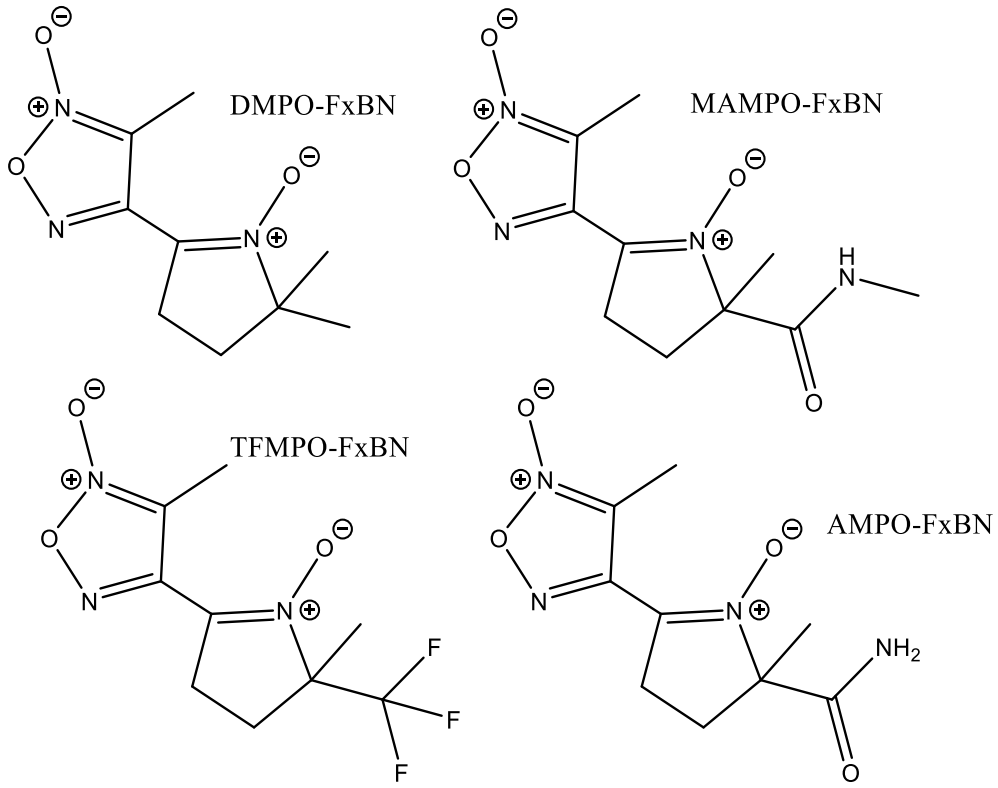

Figure 2.1. The four novel spin traps that were derived from the 4-methylfuroxynl ring of FxBN and DMPO and three of its analogs.

CHAPTER THREE

METHODOLOGY AND RESULTS

Overview

Three radical addition reactions were studied for the four novel spin traps. These three reactions were the addition of the hydroxyl radical to the C and to the O site, and the diadduct addition, which is where the hydroxyl free radical adds to both the C and the O site. The hydroxyl radical addition to the C-site, O-site, and both sites of a generic nitrone are shown in Figures 3.1-3.3 respectively.

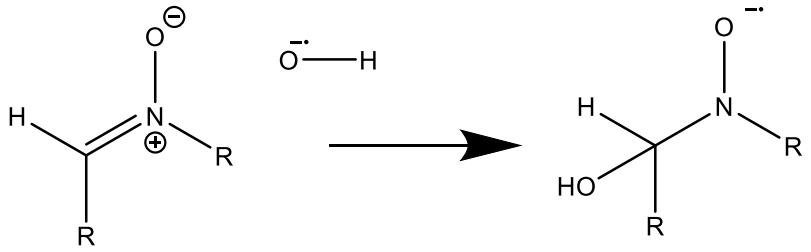

Figure 3.1. The hydroxyl radical addition to the C-Site of a generic nitrone.

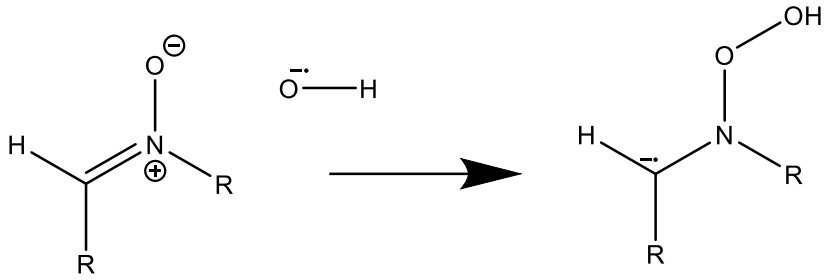

Figure 3.2. The hydroxyl radical addition to the O-Site of a generic nitrone.

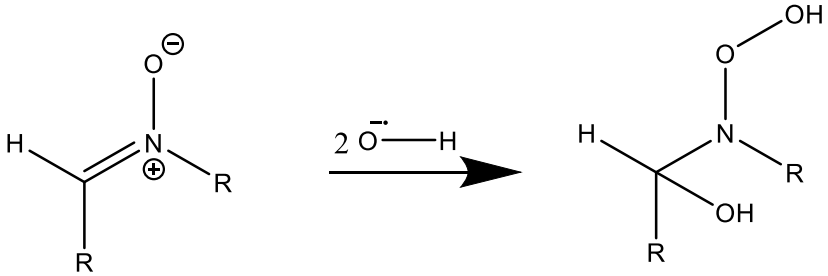

Figure 3.3. The hydroxyl radical addition to both the C and O-Site of a generic nitrone.

It should be noted that the criterion for the value of the four novel spin traps is the change in energy as the reactants form the products. If the radical addition reaction is exothermic, meaning that the change in energy is negative, the products are more stable than the reactants. Stability of the product matters since for a reaction to be favorable the product should be more stable than the reactant. The change in energy (ΔE), is:

ΔE = E of the Spin Adduct – E of the Spin Trap – nE of the hydroxyl radical (3-1)

where n is 1 for the single additions to the O or C site, and 2 for the diadduct since two hydroxyl radicals added for that reaction. The energies will be obtained by optimizing the geometries of the molecules using computational methods.

Computational Methodology

The optimized geometries for the molecules of interest were obtained using NWChem 6.8.[77] The optimized geometries were calculated for the four novel spin traps, the hydroxyl radical, and the spin adduct formed for each spin trap from the three different radical addition reactions described above. From the optimized geometries, the energy of the molecules was obtained. Two computational methods were used to optimize the geometries. One method used was the Hartree-Fock Self-Consistent-Field Theory (HF-SCF), and the other method used was Density Functional Theory (DFT). These methods were discussed earlier in the Quantum Mechanics section. Overall, both methods involve iterative approaches that try to converge on a single value for the Schrödinger wave equation. An example of this convergence in action can be seen for an HF-SCF calculation in Figure 3.4 and for a DFT calculation in Figure 3.5. The basis sets used for these methods were 6-31G*and cc-pVDZ.[78,79] In addition the B3LYP functional was used for DFT.[80] That is, in standard computational chemistry notation, the levels of theory were HF/6-31G*, HF/cc-pVDZ, DFT/B3LYP/6-31G* and DFT/B3LYP/cc-pVDZ.

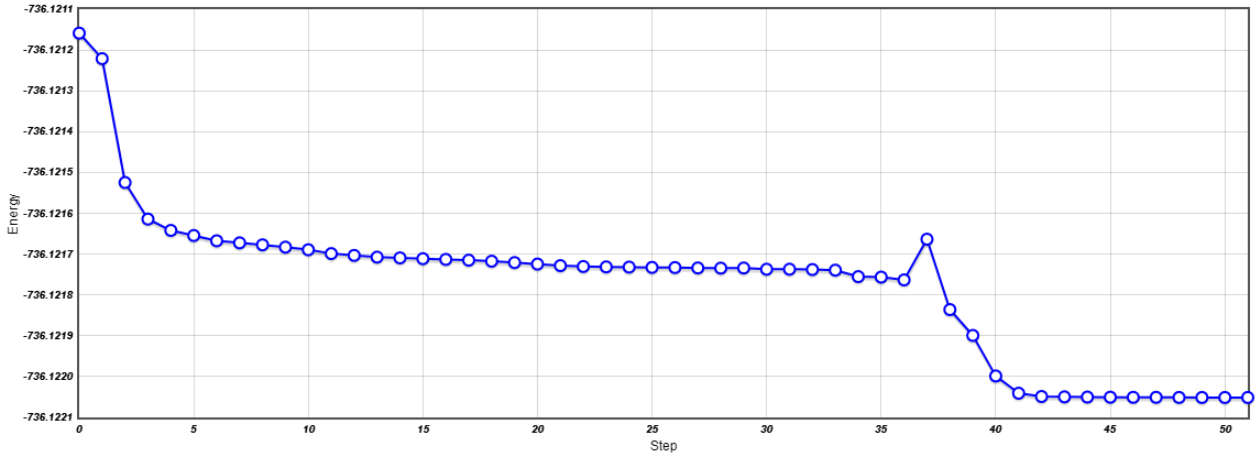

Figure 3.4. Plot of the molecular energy vs. geometry step for the optimization of the geometry for DMPO-FxBN at the HF/cc-pVDZ level of theory.

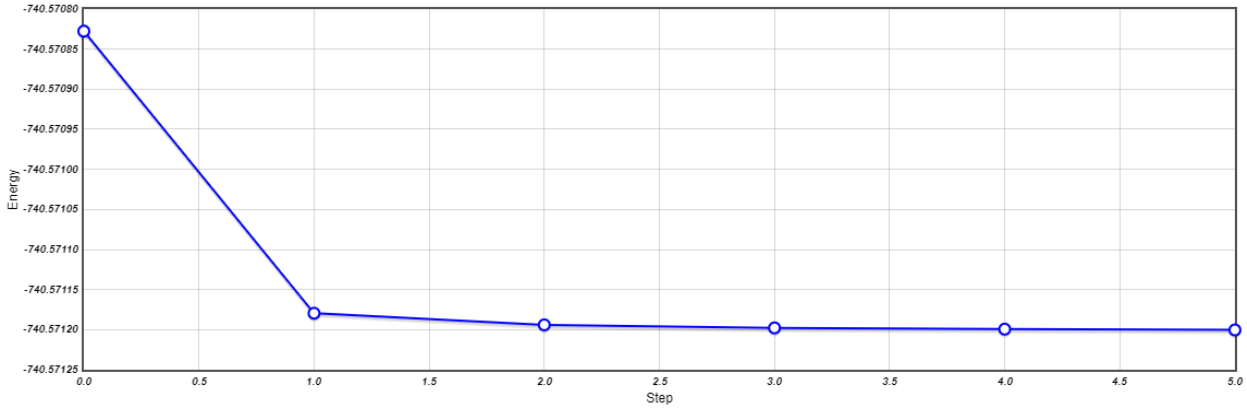

Figure 3.5. Plot of the molecular energy vs. geometry step for the optimization of the geometry for DMPO-FxBN at the DFT/B3LYP/cc-pVDZ level of theory.

Results and Discussion

The calculations ran first in this study were at the 6-31G* level of theory. From these calculated optimized geometries, the novel spin trap with the highest energy was the DMPO-FxBN. This is unsurprising since this novel spin trap had the least number of atoms in it, so it does not have as much to stabilize it as the others. TFMPO had the lowest energy. This same

trend was seen for the optimized geometries of the spin adducts at the C-site, O-site, and diadduct additions.

Table 3.1. The Energy from the Optimized Geometries at the 6-31G* Level. The energy in hartrees for the optimized geometries of the four novel spin traps and the spin adducts formed in the three different radical addition reactions are below

Energy (hartrees)					
Theory	Derivative	DMPO	TFMPO	MAMPO	AMPO
HF		-736.0597871	-1032.638537	-903.8376596	-864.8061806
DFT		-740.5176008	-1038.241183	-909.2041833	-869.9094923
	C-Site Adduct				
HF		-811.5047915	-1108.091178	-979.2669885	-940.2502366
DFT		-816.3302675	-1114.038164	-985.0143509	-945.7146684
	O-Site Adduct				
HF		-811.3841364	-1107.960389	-979.1050034	-940.1201025
DFT		-816.2559202	-1113.94442	-984.943508	-945.6414373
	Diadduct				
HF		-886.8526538	-1183.435221	-1054.617177	-1015.593131
DFT		-892.0800706	-1189.796498	-1060.766299	-1021.452156

The optimized geometry for the hydroxyl radical was calculated at the 6-31G* level. This radical was added to the structure of the four novel spin traps at the C-site, O-site, and diadduct additions to show the product of the radical addition reactions. It was used to calculate the change in energies for the free radical reactions using the following formula: ΔE = energy of spin adduct – energy of spin trap – n(energy of hydroxyl radical) where n = 1 for the C and O site additions and n = 2 for the diadduct addition. The diadduct addition is where two hydroxyl radicals added to both the C and O site. Whereas for the C and O site, only on hydroxyl radical added.

Table 3.2. Optimized Geometry of Hydroxyl Radical at the HF/6-31G* and DFT/B3LYP/6-31G* Levels of Theory. The energy calculated from the optimized geometry is below

Theory	Energy (Hartrees)
HF	-75.208616
DFT	-75.7234257

The ΔE was first calculated in hartrees, as the energies of the optimized species.. The ΔE values were then converted to kJ/mol using the conversion factor 1 hartree = 2625.5 kJ/mol. Looking at the ΔE in kJ/mol, a few trends were noticeable. One trend was that the ΔE for the C-site reactions was more exothermic than the O-site reactions. A notable calculation is of the TFMP-FxBN ΔE for the O-site spin adduct where the energy calculated was actually endothermic. This trend is to be expected since an electron-rich radical is more likely to be attracted to a carbon than an oxygen, which would make the C-site addition more likely to happen.

Table 3.3. ΔE in Hartrees for the Hydroxyl Radical Addition Reactions at the 6-31G* Level. The ΔE using the optimized geometries from above was calculated using the following formula: ΔE = energy of spin adduct – energy of spin trap – n(energy of hydroxyl radical), where n is 1 for the C-site and O-site additions and 2 for the diadduct.

Theory	Reaction	Energy (Hartrees)			
	ΔE(C-Site Spin Adduct)	DMPO	TFMPO	MAMPO	AMPO
HF		-0.23639	-0.24402	-0.22071	-0.23544
DFT		-0.08924	-0.07356	-0.08674	-0.08175
	ΔE(O-Site Spin Adduct)				
HF		-0.11573	-0.11324	-0.05873	-0.10531
DFT		-0.01489	0.020189	-0.0159	-0.00852
	Diadduct				
HF		-0.37563	-0.37945	-0.36229	-0.36972
DFT		-0.11562	-0.10846	-0.11527	-0.09581

Table 3.4. ΔE in kJ/mol for the Hydroxyl Radical Addition Reactions at the 6-31G* Level.

The energies that were calculated in Table 3.3 were converted to kJ/mol using the following conversion factor: 1 hartree = 2625.5 kJ/mol.

Theory	Reaction	Energy (kJ/mol)			
	ΔE(C-Site Spin Adduct)	DMPO	TFMPO	MAMPO	AMPO
HF		-620.638	-640.688	-579.482	-618.148
DFT		-234.302	-193.119	-227.741	-214.636
	ΔE(O-Site Spin Adduct)				
HF		-303.858	-297.301	-154.19	-276.481
DFT		-39.1034	53.00543	-41.7428	-22.3674
	Diadduct				
HF		-986.229	-996.251	-951.18	-970.696
DFT		-303.556	-284.771	-302.629	-251.555

Another trend is that the diadduct reactions are more stable than either the C-site or O-site reactions. This is also to be expected since for the diadduct two hydroxyl radicals were added to both the C and the O site, so the spin adduct is no longer a radical. Since it is no longer a radical, it should be stable. The diadduct though is not of interest in spin trapping since it lost its electron paramagnetic resonance (EPR) spectroscopy activity by no longer containing an unpaired electron.

A final general trend for the reactions is that the DMPO-FxBN analog almost always had the most stable reactions compared to the three other spin traps. There are only three exceptions. One is the TFMPO C-site addition HF calculation, the other is the MAMPO O-site addition DFT calculation, and the final exception is the TFMPO diadduct HF calculation. TFMPO would be a likely candidate to be more stable for the C-site addition since the fluorines pull electron density away from nitrone making it more susceptible to the hydroxyl radical addition. This reason could explain why it is more stable than DMPO-FxBN for two different reactions. MAMPO is 2.64

kJ/mol more stable than the DMPO-FxBN analog for that reaction. Given how small the ΔE value is, this difference is not as significant as it was for the two TFMPO exceptions where the differences were 20.05 kJ/mol and 19.98 kJ/mol respectively.

The same calculations done at the 6-31G* level of theory were done at the cc-pVDZ level of theory. The geometries were optimized for the four novel spin traps, the spin adducts of the three different radical reactions, and the hydroxyl radical. The spin trap and spin adduct with the lowest energy was the TFMPO-FxBN calculations, which was the same for the 6-31G* calculations. The highest energy for both the spin trap and spin adduct was also still the DMPO-FxBN calculations**.**

Table 3.5. The Energy from the Optimized Geometries at the cc-pVDZ Level. The energy in hartrees for the optimized geometries of the four novel spin traps and the spin adducts formed in the three different radical addition reactions are below

Energy (hartrees)					
Theory	Derivative	DMPO	TFMPO	MAMPO	AMPO
HF		-736.1220512	-1032.714974	-903.9163831	-864.8834837
DFT		-740.5711958	-1038.322244	-909.2754915	-869.9820167
	C-Site Adduct				
HF		-811.5787043	-1108.179748	-979.3578489	-940.3397811
DFT		-816.3961165	-1114.129842	-985.0971711	-945.797644
	O-Site Adduct				
HF		-811.4575482	-1108.048021	-979.1920885	-940.2093033
DFT		-816.3307671	-1114.036486	-984.9866807	-945.7256816
	Diadduct				
HF		-886.9378674	-1183.535183	-1054.719013	-1015.694321
DFT		-892.1563509	-1189.900379	-1060.862035	-1021.546100

Table 3.6. Optimized Geometry of Hydroxyl Radical at the cc-pVDZ Level. The energy calculated from the optimized geometry is below

Energy (hartrees)	
Theory	Hydroxyl Radical
HF	-75.22562788
DFT	-75.69628558

Using the optimized geometries at the cc-pVDZ level of theory, the change in energy from the reactants to the product was calculated for the three radical reactions. The overall trends were similar to the calculations at the 6-31G* level. The C-site radical addition reaction is more stable than the O-site radical addition reaction. There were no endothermic reactions for the O-site addition this time, but there were two lower values of -47.1294 kJ/mol for the TFMPO-FxBN derivative and -39.1294 kJ/mol for MAMPO-FxBN. The diadduct additions were again the most stableThe DMPO-FxBN analog had the most stable reaction for all calculations except for three, and the exceptions were the same as seen at the 6-31G* level of theory. The exceptions were TFMPO for the HF calculation at both the C-site addition and the diadduct addition and then the MAMPO DFT diadduct addition.

Table 3.7. ΔE in Hartrees for the Hydroxyl Radical Addition Reactions at the cc-pVDZ Level. The ΔE using the optimized geometries from above was calculated using the following formula: ΔE = energy of spin adduct – energy of spin trap – n(energy of hydroxyl radical), where n is 1 for the C-site and O-site additions and 2 for the diadduct.

Theory	Reaction	Energy (hartrees)			
	ΔE(C-Site Spin Adduct)	DMPO	TFMPO	MAMPO	AMPO
HF		-0.23103	-0.23915	-0.21584	-0.23067
DFT		-0.12864	-0.11131	-0.12539	-0.11934
	ΔE(O-Site Spin Adduct)				
HF		-0.10987	-0.10742	-0.05008	-0.10019
DFT		-0.063286	-0.01796	-0.0149	-0.04738
	Diadduct				
HF		-0.36456	-0.36895	-0.35137	-0.35958
DFT		-0.19258	-0.18556	-0.19397	-0.17151

Table 3.8. ΔE in kJ/mol for the Hydroxyl Radical Addition Reactions at the cc-pVDZ Level. The energies that were calculated in Table 3.3 were converted to kJ/mol using the following conversion factor: 1 hartree = 2625.5 kJ/mol.

Theory	Reaction	Energy (kJ/mol)			
	ΔE(C-Site Spin Adduct)	DMPO	TFMPO	MAMPO	AMPO
HF		-606.56	-627.88	-566.68	-605.62
DFT		-337.73	-292.25	-329.22	-313.33
	ΔE(O-Site Spin Adduct)				
HF		-288.46	-282.03	-131.48	-263.05
DFT		-166.16	-47.14	-39.129	-124.39
	Diadduct				
HF		-957.15	-968.69	-922.53	-944.08
DFT		-505.63	-487.20	-509.27	-450.30

The optimized geometries for the four novel spin trap analogs are below. These geometries are from the cc-pVDZ basis set and from the HF calculations. These geometries were inserted to show the output of the calculations in the software.

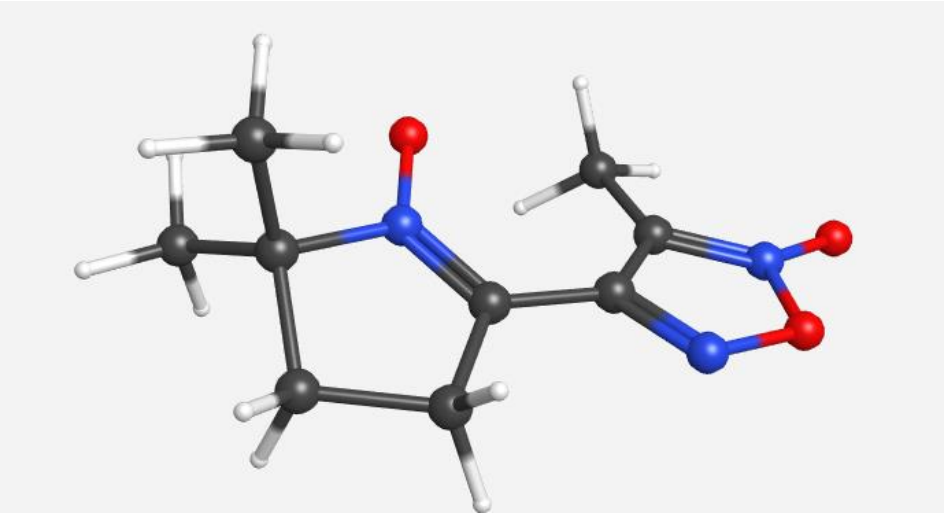

Figure 3.6. The optimized geometry of the DMPO-FxBN spin trap at the HF/cc-pVDZ level of theory.

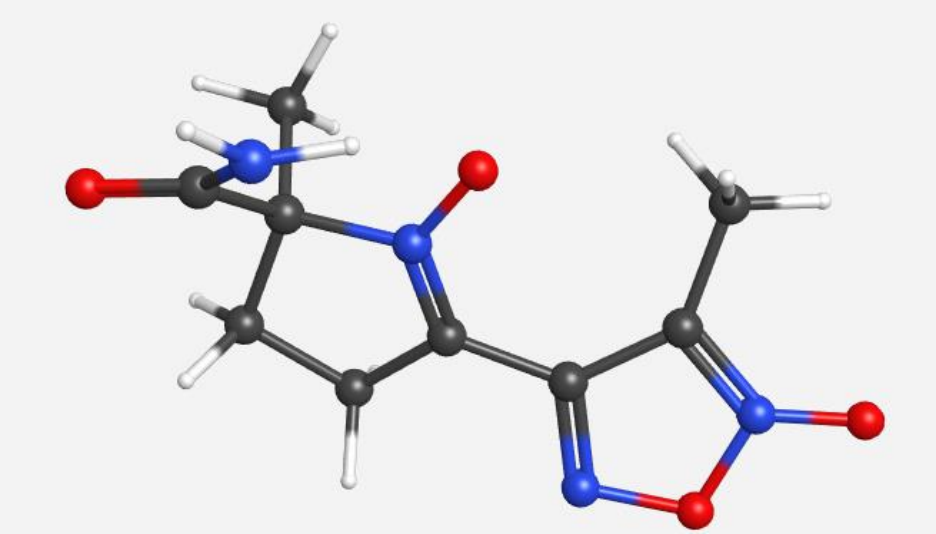

Figure 3.7. The optimized geometry of the AMPO-FxBN spin trap at the HF/cc-pVDZ level of theory.

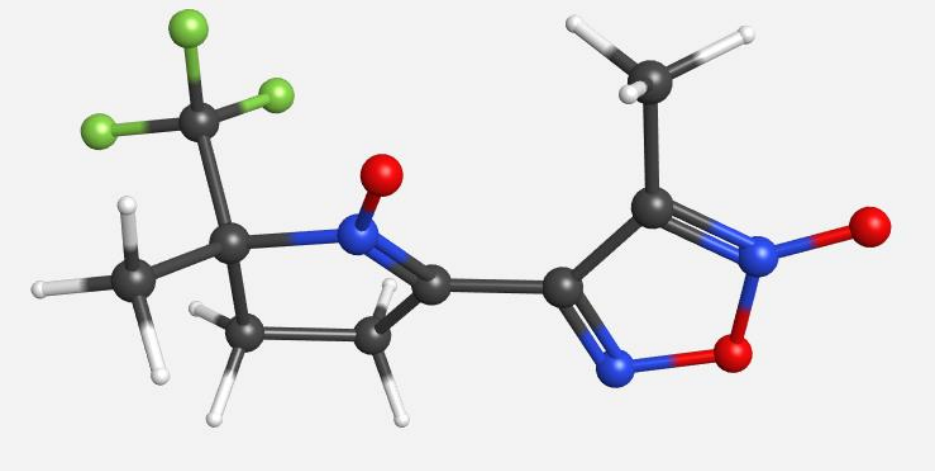

Figure 3.8. TFMPO-FxBN Novel Spin Trap Analog. The optimized geometry of the TFMPO-FxBN spin trap at the HF/cc-pVDZ level of theory.

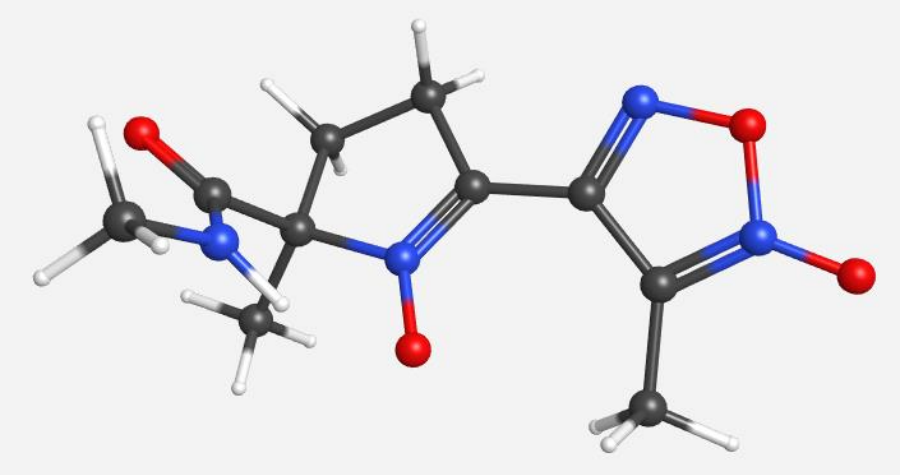

Figure 3.9. MAMPO-FxBN Novel Spin Trap Analog. The optimized geometry of the MAMPO-FxBN spin trap at the HF/cc-pVDZ level of theory.

The optimized geometries of the addition to the C and O site are also shown for the DMPO-FxBN analog along with the diadduct addition. These are also shown to illustrate the output of the calculations. In particular, to illustrate what the hydroxyl radical looks like at the C-site, O-site, and diadduct additions for one of the specific novel spin traps.

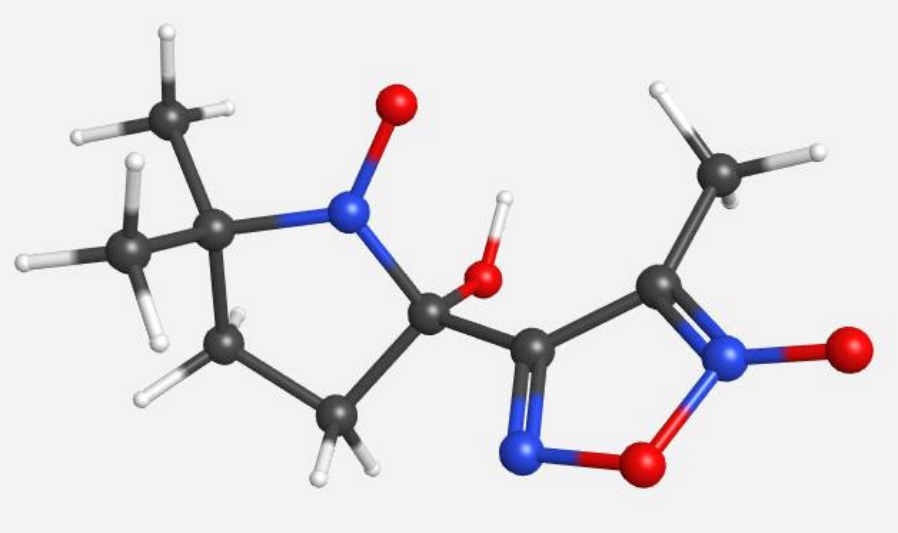

Figure 3.10. DMPO-FxBN Novel Spin Adduct C-Site Addition. The optimized geometry of the DMPO-FxBN spin adduct at the HF/cc-pVDZ level of theory. The hydroxyl radical added at the C-site of the nitrone.

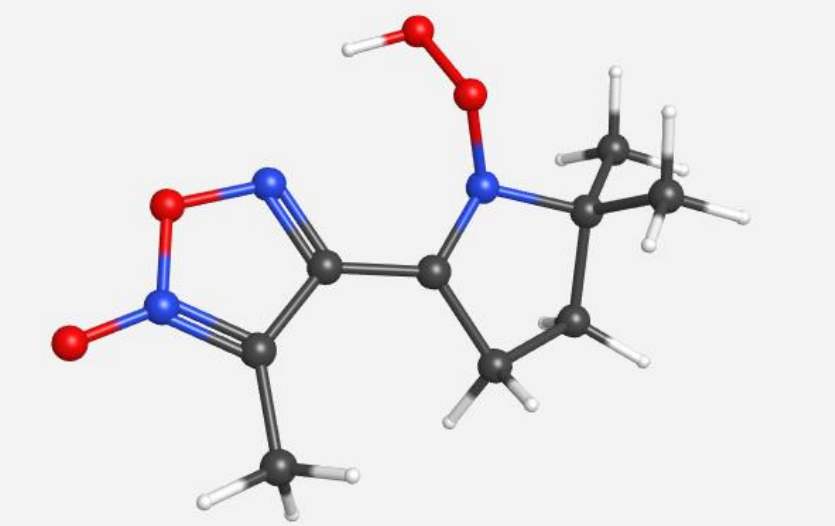

Figure 3.11. DMPO-FxBN Novel Spin Adduct O-Site Addition. The optimized geometry of the DMPO-FxBN spin adduct at the HF/cc-pVDZ level of theory. The hydroxyl radical is added at the O-site of the nitrone.

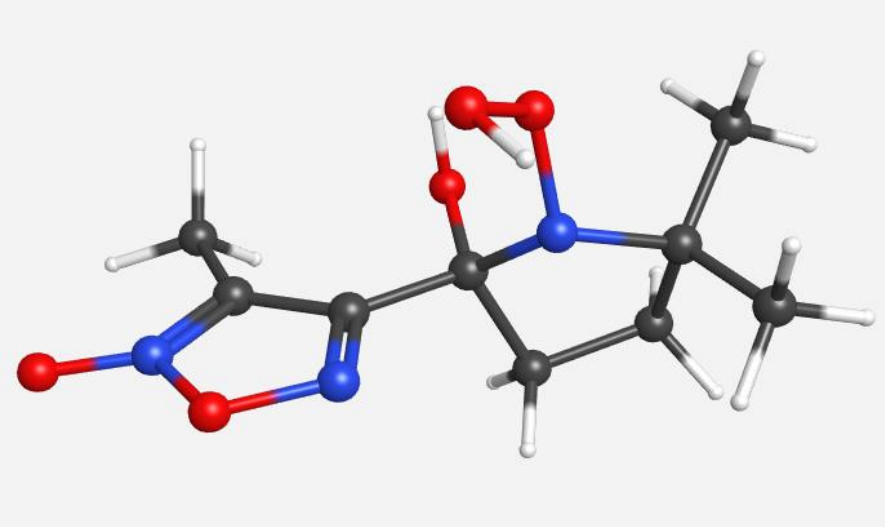

Figure 3.12. DMPO-FxBN Novel Spin Adduct Diadduct Addition. The optimized geometry of the DMPO-FxBN diadduct at the HF/cc-pVDZ level of theory. The hydroxyl radical added to both the C-site and the O-site of the nitrone.

CHAPTER FOUR

CONCLUSIONS

These four novel spin traps do produce stable spin adducts when reacted with the hydroxyl radical. The C-site addition of the hydroxyl radical is favored over the O-site addition. The diadduct is more stable than both the C and O site additions, but it is not EPR active since it was the singlet, and for spin trapping that reaction is not useful. The analog that combined the methyl-furoxynal ring from FxBN had the most stable reactions for all but three of the calculations. The Hartree-Fock and Density Functional Theory (DFT) calculations matched the overall trends for the reactions. The DFT values were lower due to the electron correlation energy. Further avenues of research would be to study the methyl-furoxynal ring on other molecules.

REFERENCES

(1) Karty, J. *Organic Chemistry: Principles and Mechanisms*, 1 edition.; W. W. Norton & Company, 2014.

(2) Phaniendra, A.; Jestadi, D. B.; Periyasamy, L. Free Radicals: Properties, Sources, Targets, and Their Implication in Various Diseases. *Indian J. Clin. Biochem.* **2015**, *30* (1), 11–26. https://doi.org/10.1007/s12291-014-0446-0.

(3) Rahman, K. Studies on Free Radicals, Antioxidants, and Co-Factors. *Clin. Interv. Aging* **2007**, *2* (2), 219–236.

(4) Turrens, J. F. Mitochondrial Formation of Reactive Oxygen Species. *J. Physiol.* **2003**, *552* (2), 335–344. https://doi.org/10.1111/j.1469-7793.2003.00335.x.

(5) Birben, E.; Sahiner, U. M.; Sackesen, C.; Erzurum, S.; Kalayci, O. Oxidative Stress and Antioxidant Defense. *World Allergy Organ. J.* **2012**, *5* (1), 9–19. https://doi.org/10.1097/WOX.0b013e3182439613.

(6) Harbour, J. R.; Chow, V.; Bolton, J. R. An Electron Spin Resonance Study of the Spin Adducts of OH and HO_2 Radicals with Nitrones in the Ultraviolet Photolysis of Aqueous Hydrogen Peroxide Solutions. *Can. J. Chem.* **1974**, *52* (20), 3549–3553. https://doi.org/10.1139/v74-527.

(7) Zweier, J.; Smith, D.; Kuppusamy, P. Measurement and Characterizationof Postischemic Free Radical Generation in the Isolated Perfused Heart. 6.

(8) Chang, R.; Goldsby, K. *Chemistry*, 12 edition.; McGraw-Hill Education: New York, NY, 2015.

(9) Valko, M.; Leibfritz, D.; Moncol, J.; Cronin, M. T. D.; Mazur, M.; Telser, J. Free Radicals and Antioxidants in Normal Physiological Functions and Human Disease. *Int. J. Biochem. Cell Biol.* **2007**, *39* (1), 44–84. https://doi.org/10.1016/j.biocel.2006.07.001.

(10) HUANG, W.-J.; ZHANG, X.; CHEN, W.-W. Role of Oxidative Stress in Alzheimer's Disease. *Biomed. Rep.* **2016**, *4* (5), 519–522. https://doi.org/10.3892/br.2016.630.

(11) Wickens, A. P. Ageing and the Free Radical Theory. *Respir. Physiol.* **2001**, *128* (3), 379–391. https://doi.org/10.1016/S0034-5687(01)00313-9.

(12) Bagchi, K.; Puri, S. Free Radicals and Antioxidants in Health and Disease. *Rev. Same Mediterr. Orient.* **1998**, *4*, 350–360.

(13) Fenton, H. J. H. LXXIII.—Oxidation of Tartaric Acid in Presence of Iron. *J. Chem. Soc. Trans.* **1894**, *65* (0), 899–910. https://doi.org/10.1039/CT8946500899.

(14) Plausible Mechanisms of the Fenton-Like Reactions, M = Fe(II) and Co(II), in the Presence of RCO2– Substrates: Are OH• Radicals Formed in the Process? | The Journal of Physical Chemistry A https://pubs.acs.org/doi/10.1021/jp512826f (accessed Feb 18, 2020).

(15) Kehrer, J. P. The Haber–Weiss Reaction and Mechanisms of Toxicity. *Toxicology* **2000**, *149* (1), 43–50. https://doi.org/10.1016/S0300-483X(00)00231-6.

(16) Haber, F.; Weiss, J.; Pope, W. J. The Catalytic Decomposition of Hydrogen Peroxide by Iron Salts. *Proc. R. Soc. Lond. Ser. - Math. Phys. Sci.* **1934**, *147* (861), 332–351. https://doi.org/10.1098/rspa.1934.0221.

(17) Lipinski, B. Hydroxyl Radical and Its Scavengers in Health and Disease https://www.hindawi.com/journals/omcl/2011/809696/ (accessed Feb 18, 2020). https://doi.org/10.1155/2011/809696.

(18) Zhu, Y.; Zhu, R.; Xi, Y.; Zhu, J.; Zhu, G.; He, H. Strategies for Enhancing the Heterogeneous Fenton Catalytic Reactivity: A Review. *Appl. Catal. B Environ.* **2019**, *255*, 117739. https://doi.org/10.1016/j.apcatb.2019.05.041.

(19) Prousek, J. Fenton Chemistry in Biology and Medicine. *Pure Appl Chem* **2007**, *79*, 2325–2338. https://doi.org/10.1351/pac200779122325.

(20) Khaliullin, R. Z.; Bell, A. T.; Head-Gordon, M. A Density Functional Theory Study of the Mechanism of Free Radical Generation in the System Vanadate/PCA/H2O2. *J. Phys. Chem. B* **2005**, *109* (38), 17984–17992. https://doi.org/10.1021/jp058162a.

(21) Sutton, H. C. Formate Oxidation Induced by a Copper Peroxo Complex Produced in Fenton-like Reactions. *J. Chem. Soc. Faraday Trans. 1 Phys. Chem. Condens. Phases* **1989**, *85* (4), 883–893. https://doi.org/10.1039/F19898500883.

(22) Khan, A. U.; Kasha, M. Singlet Molecular Oxygen in the Haber-Weiss Reaction. *Proc. Natl. Acad. Sci. U. S. A.* **1994**, *91* (26), 12365–12367. https://doi.org/10.1073/pnas.91.26.12365.

(23) Winterbourn, C. C. Toxicity of Iron and Hydrogen Peroxide: The Fenton Reaction. *Toxicol. Lett.* **1995**, *82–83*, 969–974. https://doi.org/10.1016/0378-4274(95)03532-X.

(24) Motley, C.; Mason, R. In *Biological Magnetic Resonance*; Plenum: New York, 1989; Vol. 8, pp 489–546.

(25) Becker, D. A. Highly Sensitive Colorimetric Detection and Facile Isolation of Diamagnetic Free Radical Adducts of Novel Chromotropic Nitrone Spin Trapping Agents Readily Derived from Guaiazulene. *J. Am. Chem. Soc.* **1996**, *118* (4), 905–906. https://doi.org/10.1021/ja952895z.

(26) Roessler, M. M.; Salvadori, E. Principles and Applications of EPR Spectroscopy in the Chemical Sciences. *Chem. Soc. Rev.* **2018**, *47* (8), 2534–2553. https://doi.org/10.1039/C6CS00565A.

(27) Rosen, G. M.; Beselman, A.; Tsai, P.; Pou, S.; Mailer, C.; Ichikawa, K.; Robinson, B. H.; Nielsen, R.; Halpern, H. J.; MacKerell, A. D. Influence of Conformation on the EPR Spectrum of 5,5-Dimethyl-1-Hydroperoxy-1-Pyrrolidinyloxyl: A Spin Trapped Adduct of Superoxide. *J. Org. Chem.* **2004**, *69* (4), 1321–1330. https://doi.org/10.1021/jo0354894.

(28) Gomez-Mejiba, S. E.; Zili, Z.; Della-Vedova, M. C.; Muñoz, M. D.; Chatterjee, S.; Towner, R. A.; Hensley, K.; Floyd, R. A.; Mason, R. P.; Ramirez, D. C. IMMUNO-SPIN TRAPPING FROM BIOCHEMISTRY TO MEDICINE: Advances, Challenges, and Pitfalls. *Biochim. Biophys. Acta* **2014**, *1840* (2), 722–729. https://doi.org/10.1016/j.bbagen.2013.04.039.

(29) Mason, R. P. Imaging Free Radicals in Organelles, Cells, Tissue, and in Vivo with Immuno-Spin Trapping. *Redox Biol.* **2016**, *8*, 422–429. https://doi.org/10.1016/j.redox.2016.04.003.

(30) Liu, K. J.; Miyake, M.; Panz, T.; Swartz, H. Evaluation of DEPMPO as a Spin Trapping Agent in Biological Systems. *Free Radic. Biol. Med.* **1999**, *26* (5), 714–721. https://doi.org/10.1016/S0891-5849(98)00251-2.

(31) Villamena, F. A.; Hadad, C. M.; Zweier, J. L. Kinetic Study and Theoretical Analysis of Hydroxyl Radical Trapping and Spin Adduct Decay of Alkoxycarbonyl and Dialkoxyphosphoryl Nitrones in Aqueous Media. *J. Phys. Chem. A* **2003**, *107* (22), 4407–4414. https://doi.org/10.1021/jp027829f.

(32) Bosnjakovic, A.; Schlick, S. Spin Trapping by 5,5-Dimethylpyrroline-N-Oxide in Fenton Media in the Presence of Nafion Perfluorinated Membranes: Limitations and Potential. *J. Phys. Chem. B* **2006**, *110* (22), 10720–10728. https://doi.org/10.1021/jp061042y.

(33) Gilbert, B. C.; Atherton, N. M.; Davies, M. J. *Electron Spin Resonance: Volume 14*; Royal Society of Chemistry, 2007.

(34) Haseloff, R. F.; Mertsch, K.; Rohde, E.; Baeger, I.; Grigor'ev, I. A.; Blasig, I. E. Cytotoxicity of Spin Trapping Compounds. *FEBS Lett.* **1997**, *418* (1–2), 73–75. https://doi.org/10.1016/S0014-5793(97)01349-5.

(35) Janzen, E. G.; Haire, D. Advances in Free Radical Chemistry. In *Advances in Free Radical Chemistry*; JAI Press: Greenwich, 1990; Vol. 1, p 253.

(36) Novakov, C. P.; Feierman, D.; Cederbaum, A. I.; Stoyanovsky, D. A. An ESR and HPLC-EC Assay for the Detection of Alkyl Radicals. *Chem. Res. Toxicol.* **2001**, *14* (9), 1239–1246. https://doi.org/10.1021/tx015507h.

(37) Leinisch, F.; Ranguelova, K.; DeRose, E. F.; Jiang, J.; Mason, R. P. Evaluation of the Forrester–Hepburn Mechanism As an Artifact Source in ESR Spin-Trapping. *Chem. Res. Toxicol.* **2011**, *24* (12), 2217–2226. https://doi.org/10.1021/tx2003323.

(38) Leinisch, F.; Jiang, J.; DeRose, E. F.; Khramtsov, V. V.; Mason, R. P. Investigation of Spin-Trapping Artifacts Formed by the Forrester-Hepburn Mechanism. *Free Radic. Biol. Med.* **2013**, *65*. https://doi.org/10.1016/j.freeradbiomed.2013.07.006.

(39) Hawkins, C. L.; Davies, M. J. Detection and Characterisation of Radicals in Biological Materials Using EPR Methodology. *Biochim. Biophys. Acta BBA - Gen. Subj.* **2014**, *1840* (2), 708–721. https://doi.org/10.1016/j.bbagen.2013.03.034.

(40) Boyd, S. L.; Boyd, R. J. A Theoretical Study of Spin Trapping by Nitrone: Trapping of Hydrogen, Methyl, Hydroxyl, and Peroxyl Radicals. *J. Phys. Chem.* **1994**, *98* (45), 11705–11713. https://doi.org/10.1021/j100096a013.

(41) Boyd, S. L.; Boyd, R. J. Addition vs Abstraction Reactions of the Methyl Radical with Nitrones, Alkenes, Aldehydes, and Imines. *J. Phys. Chem. A* **2001**, *105* (29), 7096–7105. https://doi.org/10.1021/jp0108115.

(42) Villamena, F. A.; Hadad, C. M.; Zweier, J. L. Comparative DFT Study of the Spin Trapping of Methyl, Mercapto, Hydroperoxy, Superoxide, and Nitric Oxide Radicals by Various Substituted Cyclic Nitrones. *J. Phys. Chem. A* **2005**, *109* (8), 1662–1674. https://doi.org/10.1021/jp0451492.

(43) Stolze, K.; Udilova, N.; Nohl, H. Lipid Radicals: Properties and Detection by Spin Trapping*. **2000**, *47*, 8.

(44) Finkelstein, E.; Rosen, G. M.; Rauckman, E. J. Spin Trapping. Kinetics of the Reaction of Superoxide and Hydroxyl Radicals with Nitrones. *J. Am. Chem. Soc.* **1980**, *102* (15), 4994–4999. https://doi.org/10.1021/ja00535a029.

(45) Makino, K.; Hagiwara, T.; Hagi, A.; Nishi, M.; Murakami, A. Cautionary Note for DMPO Spin Trapping in the Presence of Iron Ion. *Biochem. Biophys. Res. Commun.* **1990**, *172* (3), 1073–1080. https://doi.org/10.1016/0006-291X(90)91556-8.

(46) Bézière, N.; Hardy, M.; Poulhès, F.; Karoui, H.; Tordo, P.; Ouari, O.; Frapart, Y.-M.; Rockenbauer, A.; Boucher, J.-L.; Mansuy, D.; Peyrot, F. Metabolic Stability of Superoxide Adducts Derived from Newly Developed Cyclic Nitrone Spin Traps. *Free Radic. Biol. Med.* **2014**, *67*, 150–158. https://doi.org/10.1016/j.freeradbiomed.2013.10.812.

(47) Villamena, F. A.; Xia, S.; Merle, J. K.; Lauricella, R.; Tuccio, B.; Hadad, C. M.; Zweier, J. L. Reactivity of Superoxide Radical Anion with Cyclic Nitrones: Role of Intramolecular H-Bond and Electrostatic Effects. *J. Am. Chem. Soc.* **2007**, *129* (26), 8177–8191. https://doi.org/10.1021/ja0702622.

(48) Han, Y.; Tuccio, B.; Lauricella, R.; Villamena, F. A. Improved Spin Trapping Properties by β-Cyclodextrin−Cyclic Nitrone Conjugate. *J. Org. Chem.* **2008**, *73* (18), 7108–7117. https://doi.org/10.1021/jo8007176.

(49) Ortial, S.; Durand, G.; Poeggeler, B.; Polidori, A.; Pappolla, M. A.; Böker, J.; Hardeland, R.; Pucci, B. Fluorinated Amphiphilic Amino Acid Derivatives as Antioxidant Carriers: A New Class of Protective Agents. *J. Med. Chem.* **2006**, *49* (9), 2812–2820. https://doi.org/10.1021/jm060027e.

(50) Villamena, F. A.; Hadad, C. M.; Zweier, J. L. Theoretical Study of the Spin Trapping of Hydroxyl Radical by Cyclic Nitrones: A Density Functional Theory Approach. *J. Am. Chem. Soc.* **2004**, *126* (6), 1816–1829. https://doi.org/10.1021/ja038838k.

(51) Janzen, E. G.; Zhang, Y.-K.; Arimura, M. Synthesis and Spin-Trapping Chemistry of 5,5-Dimethyl-2-(Trifluoromethyl)-1-Pyrroline N-Oxide. *J. Org. Chem.* **1995**, *60* (17), 5434–5440. https://doi.org/10.1021/jo00122a021.

(52) Villamena, F. A.; Merle, J. K.; Hadad, C. M.; Zweier, J. L. Rate Constants of Hydroperoxyl Radical Addition to Cyclic Nitrones: A DFT Study. *J. Phys. Chem. A* **2007**, *111* (39), 9995–10001. https://doi.org/10.1021/jp073615s.

(53) Rosselin, M.; Tuccio, B.; Pério, P.; Villamena, Frederick. A.; Fabre, P.-L.; Durand, G. Electrochemical and Spin-Trapping Properties of Para-Substituted α-Phenyl-N-Tert-Butyl

Nitrones. *Electrochimica Acta* **2016**, *193*, 231–239. https://doi.org/10.1016/j.electacta.2016.02.038.

(54) Rosselin, M.; Choteau, F.; Zéamari, K.; Nash, K. M.; Das, A.; Lauricella, R.; Lojou, E.; Tuccio, B.; Villamena, F. A.; Durand, G. Reactivities of Substituted α-Phenyl-N-Tert-Butyl Nitrones. *J. Org. Chem.* **2014**, *79* (14), 6615–6626. https://doi.org/10.1021/jo501121g.

(55) Durand, G.; Choteau, F.; Pucci, B.; Villamena, F. A. Reactivity of Superoxide Radical Anion and Hydroperoxyl Radical with α-Phenyl-N-Tert-Butylnitrone (PBN) Derivatives. *J. Phys. Chem. A* **2008**, *112* (48), 12498–12509. https://doi.org/10.1021/jp804929d.

(56) Thomas, C. E.; Ohlweiler, D. F.; Carr, A. A.; Nieduzak, T. R.; Hay, D. A.; Adams, G.; Vaz, R.; Bernotas, R. C. Characterization of the Radical Trapping Activity of a Novel Series of Cyclic Nitrone Spin Traps. *J. Biol. Chem.* **1996**, *271* (6), 3097–3104. https://doi.org/10.1074/jbc.271.6.3097.

(57) Porcal, W.; Hernández, P.; González, M.; Ferreira, A.; Olea-Azar, C.; Cerecetto, H.; Castro, A. Heteroarylnitrones as Drugs for Neurodegenerative Diseases: Synthesis, Neuroprotective Properties, and Free Radical Scavenger Properties. *J. Med. Chem.* **2008**, *51* (19), 6150–6159. https://doi.org/10.1021/jm8006432.

(58) Barriga, G.; Olea-Azar, C.; Norambuena, E.; Castro, A.; Porcal, W.; Gerpe, A.; González, M.; Cerecetto, H. New Heteroaryl Nitrones with Spin Trap Properties: Identification of a 4-Furoxanyl Derivative with Excellent Properties to Be Used in Biological Systems. *Bioorg. Med. Chem.* **2010**, *18* (2), 795–802. https://doi.org/10.1016/j.bmc.2009.11.053.

(59) Cheng, H.-Y.; Liu, T.; Feuerstein, G.; Barone, F. C. Distribution of Spin-Trapping Compounds in Rat Blood and Brain: In Vivo Microdialysis Determination. *Free Radic. Biol. Med.* **1993**, *14* (3), 243–250. https://doi.org/10.1016/0891-5849(93)90021-L.

(60) Sack, C. A.; Socci, D. J.; Crandall, B. M.; Arendash, G. W. Antioxidant Treatment with Phenyl-α-Tert-Butyl Nitrone (PBN) Improves the Cognitive Performance and Survival of Aging Rats. *Neurosci. Lett.* **1996**, *205* (3), 181–184. https://doi.org/10.1016/0304-3940(96)12417-4.

(61) Durand, G.; Poeggeler, B.; Böker, J.; Raynal, S.; Polidori, A.; Pappolla, M. A.; Hardeland, R.; Pucci, B. Fine-Tuning the Amphiphilicity: A Crucial Parameter in the Design of Potent α-Phenyl-N-Tert-Butylnitrone Analogues. *J. Med. Chem.* **2007**, *50* (17), 3976–3979. https://doi.org/10.1021/jm0706968.

(62) Lees, K. R.; Zivin, J. A.; Ashwood, T.; Davalos, A.; Davis, S. M.; Diener, H.-C.; Grotta, J.; Lyden, P.; Shuaib, A.; Hårdemark, H.-G.; Wasiewski, W. W. NXY-059 for Acute Ischemic Stroke. *N. Engl. J. Med.* **2006**, *354* (6), 588–600. https://doi.org/10.1056/NEJMoa052980.

(63) Green, A. R.; Ashwood, T.; Odergren, T.; Jackson, D. M. Nitrones as Neuroprotective Agents in Cerebral Ischemia, with Particular Reference to NXY-059. *Pharmacol. Ther.* **2003**, *100* (3), 195–214. https://doi.org/10.1016/j.pharmthera.2003.07.003.

(64) McQuarrie, D. A.; Simon, J. D. *Physical Chemistry: A Molecular Approach*, 1 edition.; University Science Books: Sausalito, Calif, 1997.

(65) Piela, L. *Ideas of Quantum Chemistry*, 2 edition.; Elsevier, 2013.

(66) Lewars, E. G. *Computational Chemistry: Introduction to the Theory and Applications of Molecular and Quantum Mechanics*, 2nd ed. 2011 edition.; Springer: Dordrecht Netherlands ; London ; New York, 2011.

(67) Blinder, S. M. *Introduction to Quantum Mechanics: In Chemistry, Materials Science, and Biology*, 1 edition.; Academic Press: Amsterdam ; Boston, 2004.

(68) Miessler, G. L.; Fischer, P. J.; Tarr, D. A. *Inorganic Chemistry*, 5 edition.; Pearson: Boston, 2013.

(69) Born, M. Quantum Mechanics of Collision Processes (1). 25.

(70) *Classical and Quantum Information*; Elsevier, 2012. https://doi.org/10.1016/C2009-0-64195-7.

(71) Minkin, V. I. Glossary of Terms Used in Theoretical Organic Chemistry. *Pure Appl. Chem.* **1999**, *71* (10), 1919–1981. https://doi.org/10.1351/pac199971101919.

(72) Ling, S. J.; Sanny, J.; Moebs, W. The Quantum Particle in a Box. In *University Physics Volume 3*; OpenStax, 2016.

(73) Ling, S. J.; Sanny, J.; Moebs, W. The Hydrogen Atom. In *University Physics Volume 3*; OpenStax, 2016.

(74) McGibbon, R. T.; Taube, A. G.; Donchev, A. G.; Siva, K.; Hernández, F.; Hargus, C.; Law, K.-H.; Klepeis, J. L.; Shaw, D. E. Improving the Accuracy of Møller-Plesset Perturbation Theory with Neural Networks. *J. Chem. Phys.* **2017**, *147* (16), 161725. https://doi.org/10.1063/1.4986081.

(75) Sholl, D.; Steckel, J. A. *Density Functional Theory: A Practical Introduction*, 1 edition.; Wiley-Interscience, 2011.

(76) Hohenberg, P.; Kohn, W. Inhomogeneous Electron Gas. *Phys. Rev.* **1964**, *136* (3B), B864–B871. https://doi.org/10.1103/PhysRev.136.B864.

(77) Valiev, M.; Bylaska, E. J.; Govind, N.; Kowalski, K.; Straatsma, T. P.; Van Dam, H. J. J.; Wang, D.; Nieplocha, J.; Apra, E.; Windus, T. L.; de Jong, W. A. NWChem: A Comprehensive and Scalable Open-Source Solution for Large Scale Molecular Simulations. *Comput. Phys. Commun.* **2010**, *181* (9), 1477–1489. https://doi.org/10.1016/j.cpc.2010.04.018.

(78) Hehre, W. J.; Stewart, R. F.; Pople, J. A. Self-Consistent Molecular-Orbital Methods. I. Use of Gaussian Expansions of Slater-Type Atomic Orbitals. *J. Chem. Phys.* **1969**, *51* (6), 2657–2664. https://doi.org/10.1063/1.1672392.

(79) The correlation consistent composite approach (ccCA): An alternative to the Gaussian-n methods: The Journal of Chemical Physics: Vol 124, No 11 https://aip.scitation.org/doi/10.1063/1.2173988 (accessed Apr 7, 2020).

(80) Becke, A. D. Density-functional Thermochemistry. III. The Role of Exact Exchange. *J. Chem. Phys.* **1993**, *98* (7), 5648–5652. https://doi.org/10.1063/1.464913.